

# Physicochemical Properties of Choline Chloride/Acetic Acid as a Deep Eutectic Solvent and Its Binary Solutions with DMSO at 298.15 to 353.15 K

Aafia Sheikh, Athar Yaseen Khan,\* and Safeer Ahmed



Cite This: <https://doi.org/10.1021/acsomega.3c07739>



Read Online

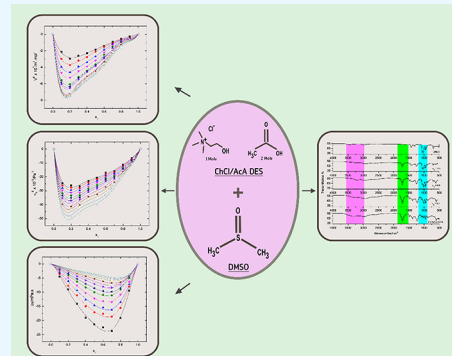
ACCESS |

Metrics & More

Article Recommendations

Supporting Information

**ABSTRACT:** Deep eutectic solvents (DESs) are considered to play an important role in green chemistry and other technological fields as an alternative to organic solvents. The present study reports measurements of density ( $\rho$ ), speed of sound ( $u$ ), dynamic viscosity ( $\eta$ ), and electrical conductivity ( $\kappa$ ) and investigates physicochemical properties of choline chloride/acetic acid (ChCl/AcA DES) and its binary mixtures with dimethyl sulfoxide (DMSO) over the entire composition and temperature (298.15–353.15 K) range. The density data are well fitted by a second-degree polynomial equation in  $T$ . DES/DMSO mixtures exhibit negative excess molar volume and isentropic compressibility deviation with a minimum in respective curves at  $x_1 \approx 0.15$  ( $x_1$  is the mole fraction of DES in the mixture), which became deeper with increasing temperature. The ChCl/AcA DES and DMSO curves for excess partial molar volume cross each other at  $x_1 \approx 0.15$ , showing that the packing effect is dominant over specific interactions. A similar behavior is observed for excess molar viscosity, showing the minima at  $x_1 \approx 0.62$ , and substantiates volumetric results. The temperature dependence of viscosity and conductivity is well described by the Vogel–Fulcher–Tammann (VFT) equation.



## 1. INTRODUCTION

A safe and healthy environment is a necessity of every society. There is a growing concern as to how to protect the environment against deterioration emerging from the large-scale use of organic solvents. This has led to an increasing demand for the application of ecofriendly processes within the framework of green and sustainable chemistry. The recognition of beneficial and interesting properties of deep eutectic solvents (DESs) has created an interest in using them and also their predecessor ionic liquids (ILs) as substitutes for conventional organic solvents.<sup>1–3</sup>

The terms DESs and ILs are interchangeably used in the literature owing to the similarity in physicochemical properties. However, they differ fundamentally from each other: DESs are systems produced by the interaction of a hydrogen bond donor (HBD) and hydrogen bond acceptor (HBA) that self-associate at a certain mole ratio resulting in a eutectic phase.<sup>4</sup> On the other hand, ILs are formed via a neutralization reaction and, thus, consist of ions. The eutectic phase is characterized by a melting point lower than either of the individual components, usually below 100 °C. Commonly desirable characteristics for selection of constituting components of DES are that they should have low toxicity and low cost and be biodegradable. On this basis, choline chloride, a quaternary ammonium salt, along with carboxylic acids and sugars, forms reasonable starting materials for synthesizing deep eutectic solvents. DESs

have emerged as a feasible alternative to ILs, although their “greenness” has been questionable at times in the context of their biocompatibility, biodegradability, and sustainability.<sup>5,6</sup> DESs can be produced at a cheaper cost and with practical ease, which makes them promising potential candidates for industrial applications compared to their traditional predecessors ILs.<sup>3</sup> They find applications in a wide variety of fields that include redox flow batteries,<sup>7–9</sup> chemical and biosensors,<sup>10,11</sup> separation processes,<sup>12</sup> drug solubility,<sup>13</sup> environmentally benign solvents in chemical synthesis, CO<sub>2</sub> capture to moderate emerging risk of climate change,<sup>14</sup> and biomass processing.<sup>15,16</sup> Although there are many combinations possible out of a large store of hydrogen bond acceptors (HBAs) and hydrogen bond donors (HBDs) for the preparation of DES, the lack of understanding of the structure–property relationship imposes a limitation on predictive designing of task-specific DESs. Choline and its derivatives are often used as HBAs due to their low toxicity and wide availability. This quaternary ammonium salt can form

Received: October 5, 2023

Revised: December 11, 2023

Accepted: December 18, 2023

**Table 1.** CAS Registry Number, Source, and Purity of the Chemicals

chemical	CAS reg. no.	source	purity	purification method
choline chloride	67-48-1	Sigma-Aldrich	≥99%	used as received
acetic acid	64-19-7	Sigma-Aldrich	≥99%	used as received
dimethylsulfoxide	67-68-5	Sigma-Aldrich	≥99%	used as received (dried by 4 Å activated molecular sieves)

**Table 2.** Density ( $\rho/\text{kg m}^{-3}$ ) of ChCl/AcA DES and ChCl/AcA DES–DMSO Mixtures in the Temperature Range  $T = 298.15$  to 353.15 K ( $x_1$  = Mole Fraction of ChCl/AcA DES) and Pressure  $p = 0.1 \text{ MPa}$ <sup>a</sup>

$x_1/T$ (K)	$\rho/\text{kg m}^{-3}$											
	298.15	303.15	308.15	313.15	318.15	323.15	328.15	333.15	338.15	343.15	348.15	353.15
0.00	1100.36	1094.11	1087.69	1081.72	1075.47	1070.25	1065.17	1059.36	1054.44	1049.52	1045.09	1040.05
0.10	1104.96	1100.29	1095.61	1090.94	1086.27	1081.60	1076.92	1072.24	1067.55	1062.86	1058.62	1053.77
0.20	1107.48	1102.97	1098.47	1093.97	1089.46	1084.97	1080.46	1075.96	1071.45	1066.94	1062.87	1058.30
0.30	1108.14	1103.68	1099.26	1094.90	1090.59	1086.07	1081.22	1077.34	1072.29	1067.82	1064.77	1060.48
0.40	1108.92	1104.55	1100.33	1096.16	1091.82	1087.49	1083.20	1079.02	1074.84	1070.77	1067.07	1063.01
0.50	1109.44	1105.07	1101.07	1097.17	1093.08	1088.99	1084.90	1081.14	1077.09	1073.22	1069.68	1065.60
0.60	1109.96	1105.66	1101.62	1097.77	1093.70	1090.09	1086.26	1082.44	1078.66	1074.97	1071.41	1067.83
0.70	1110.39	1106.42	1102.33	1098.43	1094.56	1090.96	1087.30	1083.40	1079.81	1076.19	1072.79	1069.20
0.80	1110.99	1107.26	1103.45	1099.75	1096.02	1092.46	1088.95	1085.24	1081.88	1078.53	1075.22	1071.93
0.90	1111.74	1108.27	1104.69	1101.20	1097.64	1094.23	1090.81	1087.33	1084.00	1080.60	1077.39	1074.09
1.00	1112.45	1109.12	1105.78	1102.48	1099.18	1095.89	1092.62	1089.35	1086.10	1082.84	1079.71	1076.52

<sup>a</sup>Standard uncertainties ( $u$ ) in  $T$ ,  $x_1$ ,  $p$ , and  $\rho$  are  $u(T) = 0.01 \text{ K}$ ,  $u(x_1) = 0.01$ ,  $u(p) = 10 \text{ kPa}$ , and  $u_r(\rho) = 0.003$ .

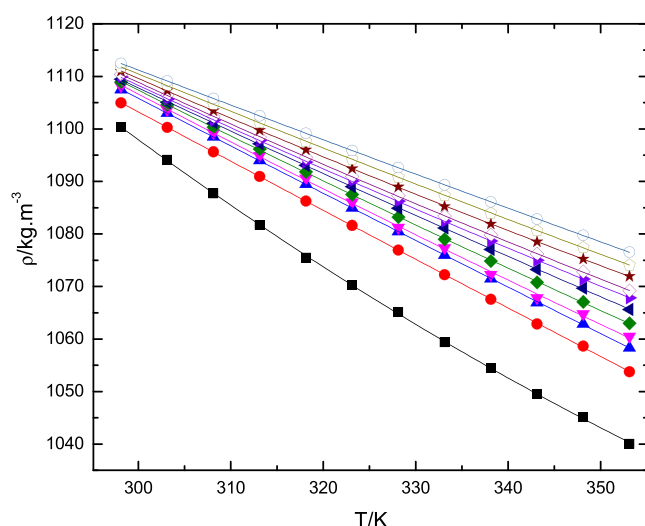


**Figure 1.** Temperature ( $T$ ) dependence of the density ( $\rho$ ) of ChCl/AcA DES–DMSO mixtures for different mole fractions of ChCl/AcA DES;  $x_1 = \blacksquare: 0.0$ ;  $\bullet: 0.1$ ;  $\blacktriangle: 0.2$ ;  $\blacktriangledown: 0.3$ ;  $\blacklozenge: 0.4$ ;  $\blacktriangleleft: 0.5$ ;  $\blacktriangleright: 0.6$ ;  $\diamond: 0.7$ ;  $\star: 0.8$ ;  $\square: 0.9$ ;  $\circ: 1.0$ .

eutectic mixtures by forming complexes with hydrogen bond donors that lower the freezing point and lattice energy.<sup>17,18</sup> They are biocompatible and degrade completely under aerobic conditions.<sup>19</sup> Acetic acid is the most important and simplest carboxylic acid and is a byproduct of fermentation. Vinegar, a food additive, is a dilute solution of acetic acid produced by the fermentation and oxidation of natural carbohydrates.<sup>20</sup> It has many industrial applications (preparation of metal acetates, plastics, cellulose acetate etc.). Acetic-acid-based DESs are extensively used in extraction and biomass pretreatment.<sup>21,22</sup> Choline-chloride-based NADES have higher levels of polarity and are therefore suitable solvents for solubilizing lignocellulose. They also have the potential to replace harsh chemicals like HCl and NaOH for the pretreatment of lignocellulosic agro-residues.<sup>23</sup>

In many cases, the relatively high viscosity of DES is an impediment in their large-scale applications.<sup>24,25</sup> There is no established approach for tuning and tailoring of viscosity and other physicochemical properties entirely based on HBA and HBD chemistry.

Addition of molecular solvents (water, dimethyl sulfoxide, alcohols, and alkanes) to DES significantly decreases its

**Table 3.** Parameters  $a_\rho$ ,  $b_\rho$ , and  $c_\rho$  Obtained by Fitting Density Data According to Eq 1 and Associated Standard Deviations

$x_1$	$a_\rho/\text{kg m}^{-3}$	$b_\rho/\text{kg m}^{-3} \text{ K}^{-1}$	$c_\rho/\text{kg m}^{-3} \text{ K}^{-2}$	$r^2$
0.00	$1820.67 \pm 2.75 \times 10^1$	$-3.53 \pm 1.69 \times 10^{-1}$	$3.75 \times 10^{-3} \pm 2.60 \times 10^{-4}$	0.9998
0.10	$1405.87 \pm 1.14 \times 10^1$	$-1.07 \pm 7.03 \times 10^{-2}$	$2.21 \times 10^{-4} \pm 1.07 \times 10^{-4}$	0.9997
0.20	$1405.73 \pm 1.09 \times 10^1$	$-1.08 \pm 6.74 \times 10^{-2}$	$2.96 \times 10^{-4} \pm 1.03 \times 10^{-4}$	0.9997
0.30	$1459.05 \pm 4.66 \times 10^1$	$-1.42 \pm 2.87 \times 10^{-1}$	$8.51 \times 10^{-4} \pm 4.40 \times 10^{-4}$	0.9993
0.40	$1445.92 \pm 1.62 \times 10^1$	$-1.37 \pm 1.00 \times 10^{-1}$	$8.26 \times 10^{-4} \pm 1.53 \times 10^{-4}$	0.9999
0.50	$1419.13 \pm 1.43 \times 10^1$	$-1.24 \pm 8.85 \times 10^{-2}$	$6.92 \times 10^{-4} \pm 1.35 \times 10^{-4}$	0.9999
0.60	$1444.68 \pm 1.14 \times 10^1$	$-1.42 \pm 7.03 \times 10^{-2}$	$1.02 \times 10^{-3} \pm 1.08 \times 10^{-4}$	0.9999
0.70	$1444.79 \pm 1.08 \times 10^1$	$-1.43 \pm 6.70 \times 10^{-2}$	$1.06 \times 10^{-3} \pm 1.02 \times 10^{-4}$	0.9999
0.80	$1440.15 \pm 7.21 \times 10^0$	$-1.43 \pm 4.43 \times 10^{-2}$	$1.11 \times 10^{-3} \pm 6.81 \times 10^{-5}$	0.9999
0.90	$1377.54 \pm 5.35 \times 10^0$	$-1.06 \pm 3.29 \times 10^{-2}$	$5.81 \times 10^{-4} \pm 5.05 \times 10^{-5}$	0.9999
1.00	$1341.26 \pm 2.37 \times 10^0$	$-0.86 \pm 1.68 \times 10^{-1}$	$3.21 \times 10^{-4} \pm 2.58 \times 10^{-5}$	1

viscosity.<sup>26–28</sup> Evaluation of thermodynamic properties of binary mixtures of DES with molecular solvents in itself is an important exercise for their use in industrial processes.<sup>29–31</sup> Dimethyl sulfoxide (DMSO) is a polar aprotic solvent of considerable commercial utility because of its dissolving power and structure that comprises two hydrophobic methyl groups and a strongly polar sulfoxide group.<sup>32</sup> The relative inertness, stability at high temperature, environmental compatibility, and low toxicity of DMSO make it a very good cosolvent apart from water, which is undoubtedly the greenest and most ideal. DMSO molecules interact with other substances through van der Waals forces and hydrogen bonding.<sup>33,34</sup> The presence of water in DES increases its mobility while maintaining its uniqueness in properties. The other important property is electrical conductivity, which is greatly affected by the presence of water content in DES.<sup>35</sup> For practical applications, the study of DES–water mixture compositions is desirable for a general understanding of their nature, optimization of performance, and knowledge of physicochemical and thermodynamic properties. Several publications on DES/water mixtures have been reported in the literature that evaluate the effect of water, but similar studies with DMSO are few.<sup>36–38</sup>

In the present study, ChCl/AcA DES is prepared from choline chloride (ChCl) and acetic acid (AcA) in mole ratio 1:2, and volumetric (density, speed of sound) and transport (dynamic viscosity, electrical conductivity) properties of its binary mixtures with DMSO are investigated in the 298.15 to 353.15 K temperature range at ambient pressure. The VFT equation is employed to fit the viscosity and electrical conductivity data, and thermodynamic properties (excess molar volume, isentropic compressibility deviation, and intermolecular free length) are evaluated from volumetric data. The functional dependence of the volumetric and transport properties on temperature and composition is discussed.

## 2. EXPERIMENTAL SECTION

**2.1. Materials.** Details of chemicals used in this work are listed below with their CAS numbers, sources, and purity (Table 1).

**2.2. Methods.** The ChCl/AcA DES was prepared following the method already reported.<sup>3,39–41</sup>

Choline chloride (HBA) and acetic acid (HBD) were mixed together in a 1:2 molar ratio in a round-bottom flask with constant stirring. The flask was fitted with a condenser, at the end of which a drying tube filled with silica gel was provided. Stirring was continued for 3 h at 323.15 to 333.15 K until a homogeneous, colorless, and transparent liquid of ChCl/AcA DES was formed. The liquid was allowed to cool to room temperature before storing it in a sealed bottle for further work. The moisture content of the final product (ChCl/AcA DES) was determined with coulometric Karl Fischer titration equipment (Mettler Toledo, V10S) using the Karl Fischer reagent (CombiNormS and methanol), which was found to be 0.06%. The moisture content of the solvent was also determined and was found to be 0.015%. The FTIR spectra of choline chloride, ChCl/AcA DES, and acetic acid were recorded on an FTIR Spectrometer (ALPHA, Bruker II). The <sup>1</sup>H NMR spectrum was recorded on a Bruker Advance 300 MHz spectrometer. These spectra are shown in Figures S1 and S3 (Supporting Information).

Binary solutions of ChCl/AcA DES and DMSO over the entire composition range were prepared by weighing DES in

airtight glass vials using an analytical balance (Shimadzu AUW220D, precision  $\pm 0.01$  mg).

The FTIR spectra of ChCl/AcA DES, DMSO, and their binary mixtures at mole fractions 0.3, 0.5, and 0.7 were also recorded and produced in Figure S2 (Supporting Information).

A density and sound velocity meter (DSA 5000, Anton Paar) was used for density ( $\rho$ ) and speed of sound ( $u$ ) measurements in the 298.15 to 353.15 K range at 5 K intervals. Calibration of the instrument was checked with air and water before measurements were made. The measuring tube was thoroughly cleaned with ultrapure water, rinsed with ethanol, and dried using a blower before injecting samples.

Viscosity measurements were performed with a viscosity module (Lovis 2000, Anton Paar) attached to a DSA 5000. The stated temperature uncertainty and repeatability factor of DSA 5000 and Module 2000 were 0.01, 0.02, 0.001, and 0.005 K, respectively. Viscosity measurements were made with capillary tubes of diameter 1.59, 1.8, and 2.5 mm (Anton Paar), which were calibrated with viscosity standards (S3, S6, N100, and N415) also from Anton Paar. Electrical conductivity was measured with a conductivity meter (Mettler Toledo Seven Compact S 230). The temperature of the conductivity cell was maintained within  $\pm 0.1$  K with a thermostated oil bath (Sci Finetech, FTCOB-S01). The standard uncertainties in mole fractions, density, speed of sound, dynamic viscosity, and conductivities were  $u(x_1) = 0.01$ ,  $u(\rho) = 3 \times 10^{-3}$  kg m<sup>-3</sup>,  $u(u) = 0.50$  m s<sup>-1</sup>,  $u(\eta) = 1.0\%$ , and  $u(\kappa) = 0.5\%$ , respectively.

## 3. RESULTS AND DISCUSSION

**3.1. Density.** The measured experimental densities ( $\rho$ /kg m<sup>-3</sup>) of ChCl/AcA DES and its binary solutions with DMSO are given in Table 2. Experimental values are fitted to a second-degree polynomial in  $T$  with eq 1, and the corresponding plots of  $\rho$  vs  $T$  are shown in Figure 1.

$$\rho = a_\rho + b_\rho T + c_\rho T^2 \quad (1)$$

The three fitting parameters  $a_\rho$ ,  $b_\rho$ , and  $c_\rho$  with their standard deviation are summarized in Table 3.

The solid lines are the best fit representations of eq 1.

$\rho$  decreases steeply with increasing temperature as a result of thermal expansion for all compositions and with increasing content of DMSO in the solution. In the last column of Table 3,  $r^2$  values are produced that are obtained by fitting the experimental density vs temperature data with a second-order polynomial equation. The  $r^2$  values indicate the success of the second-degree polynomial model used in the present case. Statistically,  $r^2$  values represent the goodness of fit, and the best fit results using a quadratic function of temperature have also been reported by other authors.<sup>30,31</sup>

The isobaric thermal expansion coefficient  $\alpha_p$  is calculated using eq 2<sup>42,43</sup> and tabulated in Table S2. Plots of  $\alpha_p$  vs  $x_1$  are shown in Figure S4.

$$\alpha_p = -\rho^{-1} \left( \frac{\partial \rho}{\partial T} \right)_p \quad (2)$$

The results show that between  $0.1 \leq x_1 \leq 0.5$ ,  $\alpha_p$  increases with increasing temperature, and then with further mole fractions, it decreases. However, beyond  $x_1 = 0.5$ , the trend in  $\alpha_p$  values is not regular. For pure components (DES and DMSO), values of  $\alpha_p$  decrease with increasing temperature.  $\alpha_p$  measures the extent to which a component expands with

**Table 4.** Excess Molar Volume ( $V^E/\text{m}^3 \text{ mol}^{-1}$ ) of ChCl/AcA DES–DMSO Mixtures at Different Temperatures<sup>a</sup>

$x_1/T$ (K)	$V^E \times 10^7/\text{m}^3 \text{ mol}^{-1}$											
	298.15	303.15	308.15	313.15	318.15	323.15	328.15	333.15	338.15	343.15	348.15	353.15
0.00	0	0	0	0	0	0	0	0	0	0	0	0
0.10	-2.133	-2.982	-3.949	-4.664	-5.564	-5.847	-6.046	-6.703	-6.802	-6.904	-7.002	-7.066
0.20	-2.951	-3.721	-4.598	-5.248	-6.061	-6.330	-6.523	-7.125	-7.230	-7.337	-7.463	-7.592
0.30	-2.589	-3.174	-3.899	-4.453	-5.183	-5.294	-5.477	-5.960	-6.140	-6.198	-6.301	-6.474
0.40	-2.301	-2.760	-3.399	-3.897	-4.405	-4.502	-4.571	-5.019	-5.098	-5.259	-5.438	-5.648
0.50	-1.848	-2.111	-2.690	-3.188	-3.659	-3.779	-3.851	-4.410	-4.456	-4.637	-4.837	-4.886
0.60	-1.406	-1.515	-1.861	-2.206	-2.478	-2.792	-2.915	-3.248	-3.355	-3.535	-3.616	-3.895
0.70	-0.916	-1.048	-1.145	-1.271	-1.477	-1.661	-1.770	-1.853	-1.974	-2.073	-2.173	-2.287
0.80	-0.540	-0.647	-0.729	-0.809	-0.910	-0.984	-1.071	-1.111	-1.272	-1.452	-1.513	-1.715
0.90	-0.277	-0.371	-0.412	-0.461	-0.475	-0.522	-0.543	-0.571	-0.631	-0.651	-0.691	-0.741
1.00	0	0	0	0	0	0	0	0	0	0	0	0

<sup>a</sup>Standard uncertainties ( $u$ ) in  $T$ ,  $x_1$ ,  $p$ , and  $\rho$  are  $u(T) = 0.01$  K,  $u(x_1) = 0.01$ ,  $u(p) = 10$  kPa, and  $u_r(\rho) = 0.003$ .

temperature, which has practical applications in various engineering processes.<sup>44</sup>

Excess molar volume  $V^E$  calculated with eq 3 is an important parameter that provides an understanding of intermolecular forces operative within the binary system.

$$V^E = \frac{x_1 M_1 + x_2 M_2}{\rho} - \left( \frac{x_1 M_1}{\rho_1} + \frac{x_2 M_2}{\rho_2} \right) \quad (3)$$

where  $x_1$  and  $x_2$  are mole fractions,  $\rho_1$  and  $\rho_2$  are densities, and  $M_1$  and  $M_2$  are molar masses, respectively, of DES and DMSO.<sup>45</sup> The molar mass of DES was calculated from eq 3a.<sup>46,47</sup>

$$M_1 = M_{\text{ChCl}} x_{\text{ChCl}} + M_{\text{AcA}} x_{\text{AcA}} \quad (3a)$$

$M_{\text{ChCl}}$  and  $M_{\text{AcA}}$  are molar masses of choline chloride and acetic acid, and  $x_{\text{ChCl}}$  and  $x_{\text{AcA}}$  are their mole fractions.

The calculated  $V^E$  values are listed in Table 4, and the corresponding plots vs  $x_1$  are given in Figure 2.

The solid lines are the best fit representation of eq 5.

For ideal mixing of components in a binary mixture, excess molar volume  $V^E$  is expected to be close to zero, for example, as observed in the case of DMSO-*n*-propyl alcohol mixture.<sup>48</sup> In the present study, the DES–DMSO binary system exhibits negative excess molar volume for all compositions, which demonstrates volume contraction on mixing the components.

Generally, excess property ( $V^E$ ,  $\kappa_S^E$ ,  $\Delta\eta$ ) values reflect the strength of intermolecular forces between the components, which could be physical (dipole–dipole interaction and dispersion forces), chemical (specific), or geometric (structural) in nature.<sup>31,49,50</sup> Physical interactions are weak forces, whereas charge transfer and hydrogen bonding interactions are stronger and lead to more efficient packing in the system and volume contraction. Structural effects arise as a result of interstices within the components producing a compact structure.<sup>51,52</sup> These contributions have complex and even opposing effects on one another.<sup>38</sup>

The variation of  $V^E$  with  $x_1$  produces a minimum located at  $x_1 \approx 0.15$  that lies in the region rich in DMSO (83.7 wt %). The magnitude of  $|V^E|$  decreases with the increase in the DES content for all compositions and temperatures investigated.

Recent studies have shown the existence of clusters in DMSO liquid and the presence of eight types of noncovalent interactions that stabilize these clusters. The CH···O hydrogen bonding interaction is the strongest, and the H···H bonding type is the weakest. Another study also proposes an SO···S

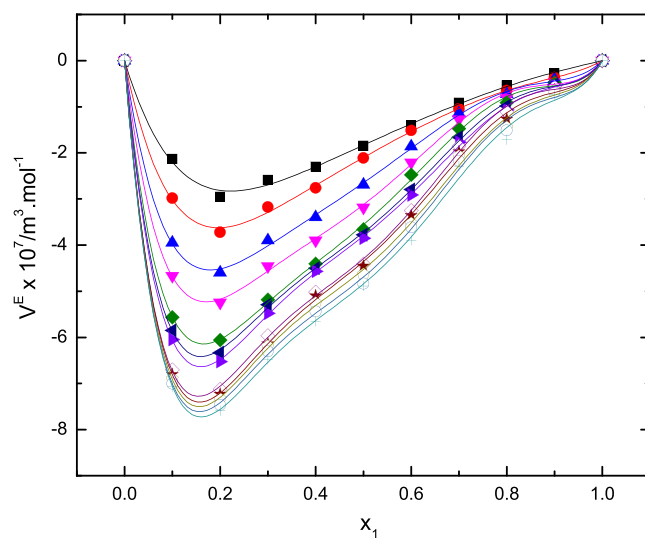


**Figure 2.** Variation of excess molar volume ( $V^E$ ) of ChCl/AcA DES–DMSO mixtures with the mole fraction of ChCl/AcA DES ( $x_1$ ) in the temperature range  $298.15 \leq T/\text{K} \leq 353.15$  (■(black): 298.15 K; ●(red): 303.15 K; ▲(blue): 308.15 K; ▼(magenta): 313.15 K; ◆(olive): 318.15 K; ▲(navy): 323.15 K; ▶(violet): 328.15 K; ◇(purple): 333.15 K; ★(wine): 338.15 K; ○(dark yellow): 343.15 K; ○(grey blue): 348.15 K; +(teal): 353.15 K).

type interaction in linear tetramers and large clusters and SO···OS type in dimers and trimers.<sup>53–56</sup>

These clusters should play an important part in the mixed state. Initially, when the DMSO concentration is high in the mixture, addition of DES produces additional strong H-bonds, leading to a more efficient packing of components in the mixed system. The other factor that gives negative values of  $V^E$  is accommodation of DES molecules into interstitial spaces among DMSO clusters particularly in the DMSO-rich region, which also produces compaction in the mixed state. As the DES content increases, DMSO structures in the mixture are disrupted. As a result, the DES–DMSO interaction is weakened, decreasing the absolute values of  $V^E$ .<sup>57</sup> The effect of increasing temperature on  $V^E$  is somewhat complex.  $|V^E|$  increases with increasing temperature, more at a low concentration of DES than at high concentrations. This could likely be explained by considering that thermal expansion creates more and larger cavities leading to more efficient accommodation of the components into each other.<sup>46</sup>

**Table 5.** Fit Parameters ( $A_j$ ) of Redlich–Kister Eq 5 for the Excess Molar Volume ( $V^E$ ) of ChCl/AcA DES–DMSO Mixtures<sup>a</sup>

T/K	$A_0$	$A_1$	$A_2$	$A_3$	$A_4$	$\sigma \times 10^{-17}$
298.15	$-7.329 \times 10^{-7} \pm 2.220 \times 10^{-8}$	$9.389 \times 10^{-7} \pm 7.266 \times 10^{-8}$	$-7.688 \times 10^{-7} \pm 2.427 \times 10^{-7}$	$6.488 \times 10^{-7} \pm 1.892 \times 10^{-7}$	$-3.419 \times 10^{-7} \pm 4.264 \times 10^{-7}$	6.477
303.15	$-8.402 \times 10^{-7} \pm 1.860 \times 10^{-8}$	$1.174 \times 10^{-6} \pm 6.087 \times 10^{-8}$	$-1.051 \times 10^{-6} \pm 2.033 \times 10^{-8}$	$1.043 \times 10^{-6} \pm 1.585 \times 10^{-7}$	$-9.061 \times 10^{-7} \pm 3.573 \times 10^{-7}$	4.546
308.15	$-1.059 \times 10^{-6} \pm 2.068 \times 10^{-8}$	$1.434 \times 10^{-6} \pm 6.767 \times 10^{-8}$	$-7.509 \times 10^{-7} \pm 2.260 \times 10^{-7}$	$1.589 \times 10^{-6} \pm 1.762 \times 10^{-7}$	$-2.235 \times 10^{-6} \pm 3.972 \times 10^{-7}$	5.619
313.15	$-1.249 \times 10^{-6} \pm 2.343 \times 10^{-8}$	$1.592 \times 10^{-6} \pm 7.668 \times 10^{-8}$	$-4.396 \times 10^{-7} \pm 2.561 \times 10^{-7}$	$2.040 \times 10^{-6} \pm 1.997 \times 10^{-7}$	$-3.314 \times 10^{-6} \pm 4.500 \times 10^{-7}$	7.213
318.15	$-1.421 \times 10^{-6} \pm 2.438 \times 10^{-8}$	$1.790 \times 10^{-6} \pm 7.980 \times 10^{-8}$	$-5.736 \times 10^{-7} \pm 2.665 \times 10^{-7}$	$2.639 \times 10^{-6} \pm 2.078 \times 10^{-7}$	$-3.906 \times 10^{-6} \pm 4.684 \times 10^{-7}$	7.813
323.15	$-1.490 \times 10^{-6} \pm 1.788 \times 10^{-8}$	$1.647 \times 10^{-6} \pm 5.851 \times 10^{-8}$	$-5.824 \times 10^{-7} \pm 1.954 \times 10^{-7}$	$3.190 \times 10^{-6} \pm 1.524 \times 10^{-7}$	$-4.170 \times 10^{-6} \pm 3.434 \times 10^{-7}$	4.201
328.15	$-1.521 \times 10^{-6} \pm 1.630 \times 10^{-8}$	$1.631 \times 10^{-6} \pm 5.336 \times 10^{-8}$	$-8.110 \times 10^{-7} \pm 1.782 \times 10^{-7}$	$3.407 \times 10^{-6} \pm 1.390 \times 10^{-7}$	$-4.023 \times 10^{-6} \pm 3.132 \times 10^{-7}$	3.493
333.15	$-1.717 \times 10^{-6} \pm 2.802 \times 10^{-8}$	$1.770 \times 10^{-6} \pm 9.171 \times 10^{-8}$	$-2.927 \times 10^{-7} \pm 3.063 \times 10^{-7}$	$3.866 \times 10^{-6} \pm 2.388 \times 10^{-7}$	$-5.330 \times 10^{-6} \pm 5.382 \times 10^{-7}$	10.33
338.15	$-1.742 \times 10^{-6} \pm 2.853 \times 10^{-8}$	$1.765 \times 10^{-6} \pm 9.338 \times 10^{-8}$	$-5.969 \times 10^{-7} \pm 3.119 \times 10^{-7}$	$3.884 \times 10^{-6} \pm 2.432 \times 10^{-7}$	$-4.994 \times 10^{-6} \pm 5.481 \times 10^{-7}$	10.69
343.15	$-1.810 \times 10^{-6} \pm 3.825 \times 10^{-8}$	$1.715 \times 10^{-6} \pm 1.251 \times 10^{-7}$	$-5.401 \times 10^{-7} \pm 4.181 \times 10^{-7}$	$4.009 \times 10^{-6} \pm 3.260 \times 10^{-7}$	$-5.126 \times 10^{-6} \pm 7.347 \times 10^{-7}$	19.22
348.15	$-1.876 \times 10^{-6} \pm 4.042 \times 10^{-8}$	$1.740 \times 10^{-6} \pm 1.322 \times 10^{-7}$	$-3.893 \times 10^{-7} \pm 4.418 \times 10^{-7}$	$4.024 \times 10^{-6} \pm 3.445 \times 10^{-7}$	$-5.406 \times 10^{-6} \pm 7.7641 \times 10^{-7}$	21.46
353.15	$-1.936 \times 10^{-6} \pm 4.609 \times 10^{-8}$	$1.731 \times 10^{-6} \pm 1.508 \times 10^{-7}$	$-6.264 \times 10^{-7} \pm 5.039 \times 10^{-7}$	$4.027 \times 10^{-6} \pm 3.929 \times 10^{-7}$	$-5.042 \times 10^{-6} \pm 8.854 \times 10^{-7}$	27.92

<sup>a</sup>The fourth-degree Redlich–Kister polynomial equation satisfactorily reproduces  $V^E$  values calculated using experimental density data as shown by the solid lines in Figure 2. Thus, a fairly good correlation is achieved between the theoretical and experimentally determined values.

**Table 6.** Speed of Sound ( $u/\text{m s}^{-1}$ ) of ChCl/AcA DES–DMSO mixtures as a Function of Temperature  $T = 298.15$  to  $353.15$  K and Pressure  $p = 0.1$  MPa<sup>a</sup>

$x_1/T$ (K)	$u/(\text{m s}^{-1})$											
	298.15	303.15	308.15	313.15	318.15	323.15	328.15	333.15	338.15	343.15	348.15	353.15
0.00	1455.1	1438.4	1421.6	1404.9	1388.0	1371.3	1354.5	1337.7	1320.9	1304.1	1287.4	1270.6
0.10	1514.9	1498.6	1482.4	1466.2	1450.1	1433.9	1417.9	1401.9	1386.0	1370.2	1354.3	1338.4
0.20	1536.0	1520.1	1504.3	1488.5	1472.6	1456.8	1441.1	1425.3	1409.7	1394.0	1378.4	1363.0
0.30	1558.0	1542.1	1526.4	1510.7	1494.9	1479.1	1463.5	1447.8	1432.2	1416.7	1401.2	1385.8
0.40	1570.9	1555.4	1539.8	1524.4	1508.9	1493.4	1477.8	1462.3	1446.9	1431.6	1416.3	1401.1
0.50	1587.9	1572.9	1557.8	1542.8	1527.9	1513.3	1498.2	1483.7	1470.0	1455.5	1442.8	1428.6
0.60	1602.4	1587.7	1573.0	1558.3	1543.5	1528.8	1514.3	1500.7	1487.9	1475.3	1460.6	1446.0
0.70	1623.5	1609.2	1595.0	1581.0	1566.8	1552.8	1538.6	1524.5	1510.3	1496.3	1482.6	1470.0
0.80	1636.5	1622.7	1608.8	1594.9	1581.0	1567.2	1553.3	1539.4	1525.3	1511.4	1497.4	1483.4
0.90	1649.0	1636.1	1622.9	1609.5	1596.1	1583.1	1570.1	1556.8	1543.5	1530.0	1516.6	1503.3
1.00	1658.1	1645.1	1632.3	1619.3	1606.2	1593.3	1580.3	1567.3	1554.3	1541.4	1528.3	1515.4

<sup>a</sup>Standard uncertainties ( $u$ ) in  $T$ ,  $x$ ,  $P$ , and  $u$  are  $u(T) = 0.01$  K,  $u(x_1) = 0.01$ ,  $u(P) = 10$  kPa, and  $u_r(u) = 0.5$ .

In the understanding of the solute–solute and solute–solvent interaction behavior in solutions, partial molar properties are important parameters. The calculation of the apparent molar volume  $V_{\phi,i}$  (eq 4) and partial molar volume  $\bar{V}_i$  (eq 6) for individual components of the binary system is evaluated [ $i = 1$  (ChCl/AcA DES),  $i = 2$  (DMSO)].

$$V_{\phi,i} = V_{m,i} + \frac{V^E}{x_i} \quad (4)$$

$V_{m,i}$  is the molar volume of the pure component  $i$ . Tables S3 and S4 (Supporting Information) summarize the calculated apparent molar volumes of the components (DES and DMSO) at different temperatures. The values of  $V_{\phi,i}$  are positive for both DES and DMSO, indicating strong solvent–solute interactions in binary mixtures. A representative plot of  $V_{\phi,1}$  values of ChCl/AcA DES + DMSO mixtures as a function of  $x_1$  is shown in Figure S5 (Supporting Information).

The excess molar volume  $V^E$  data are fitted to the Redlich–Kister polynomial (eq 5).<sup>58,59</sup> The excess molar property ( $Y^E = V^E, \kappa_S^E, \Delta\eta$ ) in the combined Redlich–Kister (CNIBS/R-K) model at constant temperature can be expressed by eq 5.

$$Y^E = x_{\text{DES}}x_{\text{DMSO}} \sum_{j=0}^k A_j (x_{\text{DES}} - x_{\text{DMSO}})^j \quad (5)$$

where  $A_j$ 's are coefficients that are adjustable parameters obtainable by regression analysis and collected in Table 5 and  $j$  is the degree of polynomial equation.

The partial and excess partial molar volumes  $\bar{V}_i$ 's of individual components were calculated using eqs 6 and 7, respectively,<sup>26</sup> and the results are listed in Tables S5–S8 (Supporting Information). As an example, Figure S6 (Supporting Information) shows the  $\bar{V}_i^E$  of ChCl/AcA DES and DMSO vs  $x_1$  at 298 K. It is interesting to note that the two curves cross each other at  $x_1 \approx 0.15$ , where  $V^E$  exhibits its minimum. The temperature dependence of  $\bar{V}_i^E$  suggests that the packing effect is dominant over specific interactions.

$$\bar{V}_i = V_{m,i} + V^E + (1-x)\left(\frac{\partial V^E}{\partial x_i}\right)_{P,T} \quad (6)$$

$$\bar{V}_i^E = \bar{V}_i - V_{m,i} \quad (7)$$

The solute–solvent interactions fade at the limit of infinite dilution. The calculation of partial molar properties at infinite dilution provides useful information about solute–solvent interactions independent of the composition effect. The partial molar volume at infinite dilution for ChCl/AcA DES ( $\bar{V}_1^\infty$ ) and DMSO ( $\bar{V}_2^\infty$ ) can be calculated by using eqs 8 and 9, respectively.

$$\bar{V}_1^\infty = V_{m,1} + \sum_{i=1}^n A_i (-1)^i \quad (8)$$

$$\bar{V}_2^\infty = V_{m,2} + \sum_{i=2}^n A_i \quad (9)$$

The calculated values from eqs 8 and 9 are listed in Table S9 (Supporting Information). The partial molar volume at infinite dilution supports the conclusion that the packing effect is dominant over specific interactions.

**3.2. Speed of Sound.** Apart from volumetric properties, acoustic properties of binary solutions also contribute toward investigating thermophysical properties and in the understanding of intermolecular interactions forces between components.<sup>60,61</sup> The speed of sound,  $u$ , of DES and its mixtures with molecular liquids can be determined experimentally with precision with DSA5000. The measurement of the property has its significance as it relates to other properties such as density, thermal conductivity, isentropic and isothermal compressibility, and heat capacity.<sup>62</sup> Experimentally determined values of  $u$  are given in Table 6 and plotted as a function of T in Figure 3.

The speed of sound decreases with increasing temperature due to the slowing down of the sound waves in the medium that has become less dense.<sup>63–65</sup> The effect of increasing the DES content in the mixture results in increasing  $u$  because the medium has now become denser. The effects of varying

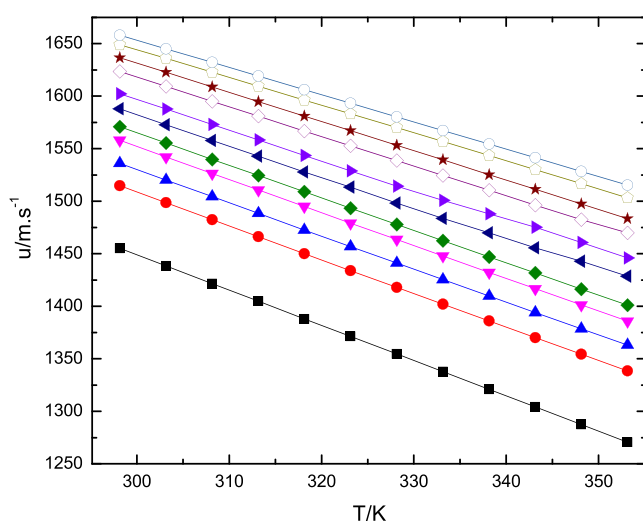


**Figure 3.** Temperature dependence of speed of sound ( $u$ ) of the binary mixture ChCl/AcA DES + DMSO with varying  $x_1$  = (■(black), 0.0; ●(red), 0.1; ▲(blue):0.2; ▼(magenta): 0.3; ◆(olive), 0.4; ▲(navy), 0.5; ▶(violet), 0.6; ◇(purple), 0.7; ★(wine), 0.8; ◇(dark yellow), 0.9; ○(grey blue): 1.00).

temperature and composition on the speed of sound and density are analogous.

The Newton–Laplace equation (eq 10) enables the calculation of isentropic compressibility,  $\kappa_s$ , of the binary mixture from the density and speed of sound data.<sup>66</sup> The results are reported in Table 7 as functions of temperature and compositions. The “compressibility” parameter reflects the relative change in volume of the fluid as a result of the corresponding change in pressure. The information obtainable from the experimentally determined isentropic compressibility is about the available free space in the liquid structure.<sup>67</sup>

$$\kappa_s = \frac{1}{\rho \cdot u^2} \quad (10)$$

$\kappa_s$  is considered to have contributions from solvent intrinsic and solute intrinsic isentropic compressibilities. The  $\kappa_s$  value of neat DMSO is  $429.2 \times 10^{-12}$  Pa<sup>-1</sup> at 298.15 K. At  $x_1 = 0.1$ , there is large decrease of  $45.1 \times 10^{-12}$  Pa<sup>-1</sup> in  $\kappa_s$  value compared to neat DMSO, which indicates the tightening of the DES–DMSO structure in the mixture.<sup>40</sup> The decrease in  $\kappa_s$  values continues with increasing DES content for all compositions and temperatures. The increase in  $\kappa_s$  with increasing temperature over the entire range suggests the loosening of the tight structure.<sup>68</sup> The temperature dependence of  $\kappa_s$  for ChCl/AcA DES is shown in Figure 4.

The isentropic compressibility deviation,  $\kappa_s^E$ , can be calculated from the following eq 11:

$$\kappa_s^E = \kappa_s - \sum_i x_i \kappa_{s,i} \quad (11)$$

where  $x_i$  and  $\kappa_{s,i}$  are mole fractions and isentropic compressibility of component  $i$ , respectively.

The calculated values of  $\kappa_s^E$  are collected in Table 8 as functions of composition and temperature. The plot of  $\kappa_s^E$  vs  $x_1$  is shown in Figure 5. The  $\kappa_s^E$  parameter provides insight into the nature of the interaction within the binary liquid system. The calculated  $\kappa_s^E$  values are all negative over the entire range of temperatures and compositions investigated. The negative values of  $\kappa_s^E$  are attributed to specific and structural interactions in the liquid mixture.<sup>69,70</sup> The shapes of  $\kappa_s^E$  vs  $x_1$  (Figure 5) and  $V^E$  vs  $x_1$  (Figure 2) are very similar in nature. The minimum in Figure 5 occurs at  $x_1 = 0.15$ ,<sup>65</sup> which is exactly the same as found in the  $V^E$  vs  $x_1$  plot. Moreover, the absolute values of  $\kappa_s^E$  decrease at all compositions and temperatures. Further, as the temperature is increased, absolute  $\kappa_s^E$  values increase, again more at low concentrations of DES than at high concentrations. These trends are like those observed for the excess molar volume property and deserve the same explanation.

The isentropic compressibility deviation ( $\kappa_s^E$ ) is fitted with Redlich–Kister eq 5, and the fitting parameters are tabulated in Table 9.

The solid lines are the best fit representation of eq 5.

Intermolecular free length,  $L_f$  is calculated from eq 12. This acoustic property is used to study intermolecular interaction and its influence on structural arrangement.<sup>71</sup> It specifies the distance between the surfaces of neighboring molecules.<sup>72</sup>

$$L_f = \frac{K}{u \rho^{0.5}} \quad (12)$$

where  $K$  is Jacobson's constant,<sup>73</sup>  $\rho$  (kg m<sup>-3</sup>) is density, and  $u$  (m s<sup>-1</sup>) is the speed of sound. The calculated values of  $L_f$  are shown in Table 10 and plotted in Figure 6 against  $x_1$ .  $L_f$  decreases with an increasing concentration of DES but

**Table 7.** Isentropic Compressibility ( $\kappa_s/\text{Pa}^{-1}$ ) of ChCl/AcA DES–DMSO Mixtures as a Function of Temperature ( $T$ )<sup>a</sup>

$x_1/T$ (K)	$\kappa_s \times 10^{12}/\text{Pa}^{-1}$											
	298.15	303.15	308.15	313.15	318.15	323.15	328.15	333.15	338.15	343.15	348.15	353.15
0.00	429.2	441.8	454.9	468.4	482.6	496.9	511.7	527.5	543.5	560.3	577.3	595.6
0.10	394.4	404.7	415.3	426.4	437.8	449.7	461.9	474.5	487.6	501.1	515.0	529.8
0.20	382.7	392.4	402.3	412.6	423.2	434.3	445.7	457.5	469.7	482.3	495.2	508.6
0.30	371.8	381.0	390.4	400.2	410.3	420.9	431.8	442.8	454.6	466.6	478.3	491.0
0.40	365.4	374.2	383.3	392.6	402.3	412.3	422.7	433.4	444.4	455.7	467.2	479.2
0.50	357.5	365.8	374.2	382.9	391.9	401.0	410.6	420.2	429.7	439.8	449.1	459.8
0.60	350.9	358.8	366.9	375.2	383.8	392.5	401.5	410.2	418.8	427.4	437.5	447.9
0.70	341.7	349.0	356.6	364.2	372.1	380.1	388.5	397.2	406.0	415.1	424.1	432.9
0.80	336.1	343.0	350.1	357.5	365.0	372.7	380.6	388.9	397.3	405.9	414.8	423.9
0.90	330.8	337.1	343.7	350.6	357.6	364.6	371.9	379.5	387.2	395.3	403.5	412.0
1.00	327.0	333.1	339.4	345.9	352.7	359.5	366.5	373.7	381.1	388.7	396.6	404.5

<sup>a</sup>Standard uncertainties ( $u$ ) in  $T$ ,  $x$ ,  $P$ , and  $u$  are  $u(T) = 0.01$  K,  $u(x_1) = 0.01$ ,  $u(P) = 10$  kPa, and  $u_r(u) = 0.5$ .

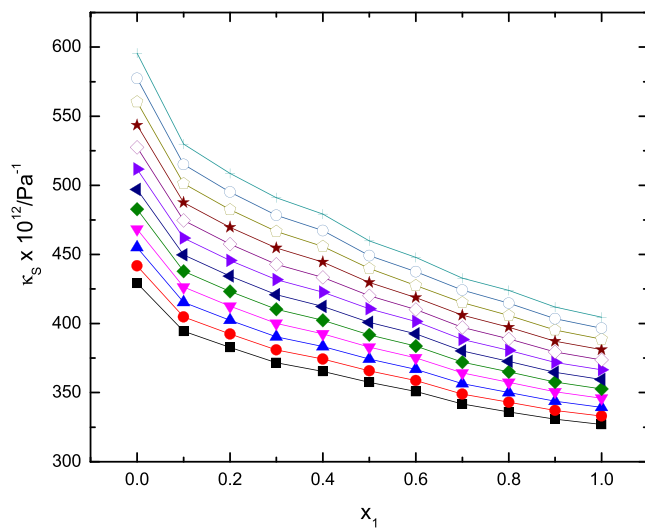


**Figure 4.** Isentropic compressibility ( $\kappa_s \times 10^{12}/\text{Pa}^{-1}$ ) of ChCl/AcA DES–DMSO mixtures as a function of  $x_1$  in the temperature range  $298.15 \leq T/\text{K} \leq 353.15$  (■(black)): 298.15 K; (●(red)): 303.15 K; (▲(blue)): 308.15 K; (▼(magenta)): 313.15 K; (◆(olive)): 318.15 K; (◀(navy)): 323.15 K; (▶(violet)): 328.15 K; (◊(purple)): 333.15 K; (★(wine)): 338.15 K; (◇(dark yellow)): 343.15 K; (○(grey blue)): 348.15 K; (+(teal)) : 353.15 K.

increases as the temperature is increased. The decreasing  $L_f$  values indicate the formation of more compact structures as

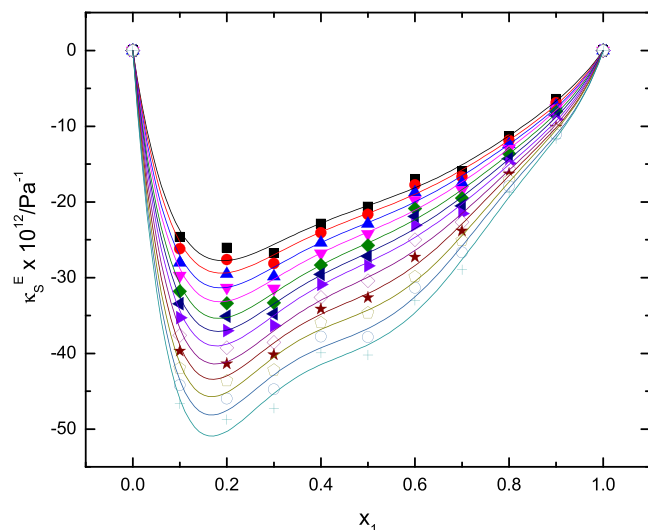


**Figure 5.** Isentropic compressibility deviation ( $\kappa_E^S \times 10^{12}/\text{Pa}^{-1}$ ) of ChCl/AcA DES–DMSO mixtures as a function of  $x_1$  in the temperature range  $298.15 \leq T/\text{K} \leq 353.15$  (■(black)): 298.15 K; (●(red)): 303.15 K; (▲(blue)): 308.15 K; (▼(magenta)): 313.15 K; (◆(olive)): 318.15 K; (◀(navy)): 323.15 K; (▶(violet)): 328.15 K; (◊(purple)): 333.15 K; (★(wine)): 338.15 K; (◇(dark yellow)): 343.15 K; (○(grey blue)): 348.15 K; (+(teal)) : 353.15 K.

**Table 8.** Isentropic compressibility deviation ( $\kappa_E^S/\text{Pa}^{-1}$ ) of ChCl/AcA DES–DMSO Mixtures at Different Temperatures ( $T$ )<sup>a</sup>

$x_1/T$ (K)	$\kappa_E^S \times 10^{12}/\text{Pa}^{-1}$											
	298.15	303.15	308.15	313.15	318.15	323.15	328.15	333.15	338.15	343.15	348.15	353.15
0.00	0	0	0	0	0	0	0	0	0	0	0	0
0.10	-24.64	-26.20	-28.03	-29.75	-31.83	-33.47	-35.31	-37.61	-39.71	-41.96	-44.21	-46.67
0.20	-26.04	-27.64	-29.54	-31.32	-33.39	-35.09	-37.00	-39.28	-41.37	-43.63	-46.00	-48.74
0.30	-26.78	-28.16	-29.84	-31.44	-33.33	-34.79	-36.32	-38.56	-40.18	-42.20	-44.76	-47.26
0.40	-22.90	-24.09	-25.42	-26.81	-28.36	-29.58	-30.89	-32.60	-34.16	-35.96	-37.81	-39.95
0.50	-20.64	-21.67	-22.93	-24.22	-25.75	-27.20	-28.45	-30.44	-32.65	-34.67	-37.86	-40.23
0.60	-17.00	-17.77	-18.77	-19.75	-20.86	-21.93	-23.08	-25.02	-27.30	-29.89	-31.36	-33.04
0.70	-15.96	-16.70	-17.49	-18.42	-19.50	-20.54	-21.55	-22.67	-23.86	-25.12	-26.69	-28.98
0.80	-11.33	-11.88	-12.41	-12.94	-13.63	-14.27	-14.90	-15.61	-16.29	-17.10	-17.92	-18.77
0.90	-6.397	-6.903	-7.285	-7.623	-8.044	-8.553	-9.099	-9.594	-10.12	-10.51	-11.12	-11.64
1.00	0	0	0	0	0	0	0	0	0	0	0	0

<sup>a</sup>Standard uncertainties ( $u$ ) in  $T$ ,  $x$ ,  $P$ , and  $u$  are  $u(T) = 0.01$  K,  $u(x_1) = 0.01$ ,  $u(P) = 10$  kPa, and  $u_r(u) = 0.5$ .

**Table 9.** Fit Parameters ( $A_i$ ) of the Redlich–Kister Equation (Eq 5) for the Isentropic Compressibility Deviation ( $\kappa_S^E$ ) of ChCl/AcA DES–DMSO Mixtures

T/K	$A_0$	$A_1$	$A_2$	$A_3$	$A_4$	$\sigma \times 10^{-24}$
298.15	$-8.200 \times 10^{-11} \pm 3.038 \times 10^{-12}$	$4.401 \times 10^{-11} \pm 9.945 \times 10^{-12}$	$-7.921 \times 10^{-11} \pm 3.322 \times 10^{-11}$	$1.162 \times 10^{-10} \pm 2.590 \times 10^{-11}$	$-8.821 \times 10^{-11} \pm 5.837 \times 10^{-11}$	1.213
303.15	$-8.607 \times 10^{-11} \pm 3.121 \times 10^{-12}$	$4.713 \times 10^{-11} \pm 1.021 \times 10^{-11}$	$-8.208 \times 10^{-11} \pm 3.411 \times 10^{-11}$	$1.226 \times 10^{-10} \pm 2.660 \times 10^{-11}$	$-1.016 \times 10^{-10} \pm 5.994 \times 10^{-11}$	1.280
308.15	$-9.095 \times 10^{-11} \pm 3.184 \times 10^{-12}$	$5.061 \times 10^{-11} \pm 1.042 \times 10^{-11}$	$-8.534 \times 10^{-11} \pm 3.481 \times 10^{-11}$	$1.330 \times 10^{-10} \pm 2.714 \times 10^{-11}$	$-1.144 \times 10^{-10} \pm 6.116 \times 10^{-11}$	1.332
313.15	$-9.594 \times 10^{-11} \pm 3.318 \times 10^{-12}$	$5.335 \times 10^{-11} \pm 1.085 \times 10^{-11}$	$-8.844 \times 10^{-11} \pm 3.627 \times 10^{-11}$	$1.435 \times 10^{-10} \pm 2.828 \times 10^{-11}$	$-1.249 \times 10^{-10} \pm 6.373 \times 10^{-11}$	1.447
318.15	$-1.016 \times 10^{-10} \pm 3.535 \times 10^{-12}$	$5.634 \times 10^{-11} \pm 1.157 \times 10^{-11}$	$-9.257 \times 10^{-11} \pm 3.864 \times 10^{-11}$	$1.561 \times 10^{-10} \pm 3.013 \times 10^{-11}$	$-1.379 \times 10^{-10} \pm 6.790 \times 10^{-11}$	1.642
323.15	$-1.069 \times 10^{-10} \pm 3.646 \times 10^{-12}$	$5.738 \times 10^{-11} \pm 1.193 \times 10^{-11}$	$-9.276 \times 10^{-11} \pm 3.986 \times 10^{-11}$	$1.673 \times 10^{-10} \pm 3.108 \times 10^{-11}$	$-1.541 \times 10^{-10} \pm 7.003 \times 10^{-11}$	1.747
328.15	$-1.119 \times 10^{-10} \pm 3.633 \times 10^{-12}$	$5.887 \times 10^{-11} \pm 1.189 \times 10^{-11}$	$-9.601 \times 10^{-11} \pm 3.971 \times 10^{-11}$	$1.798 \times 10^{-10} \pm 3.097 \times 10^{-11}$	$-1.688 \times 10^{-10} \pm 6.978 \times 10^{-11}$	1.735
333.15	$-1.197 \times 10^{-10} \pm 3.617 \times 10^{-12}$	$6.073 \times 10^{-11} \pm 1.183 \times 10^{-11}$	$-9.143 \times 10^{-11} \pm 3.954 \times 10^{-11}$	$1.974 \times 10^{-10} \pm 3.083 \times 10^{-11}$	$-1.944 \times 10^{-10} \pm 6.947 \times 10^{-11}$	1.719
338.15	$-1.283 \times 10^{-10} \pm 3.304 \times 10^{-12}$	$5.820 \times 10^{-11} \pm 1.081 \times 10^{-11}$	$-7.563 \times 10^{-11} \pm 3.611 \times 10^{-11}$	$2.210 \times 10^{-10} \pm 2.816 \times 10^{-11}$	$-2.347 \times 10^{-10} \pm 6.346 \times 10^{-11}$	1.434
343.15	$-1.371 \times 10^{-10} \pm 3.083 \times 10^{-12}$	$5.612 \times 10^{-11} \pm 1.009 \times 10^{-11}$	$-6.765 \times 10^{-11} \pm 3.370 \times 10^{-11}$	$2.463 \times 10^{-10} \pm 2.628 \times 10^{-11}$	$-2.616 \times 10^{-10} \pm 5.922 \times 10^{-11}$	1.249
348.15	$-1.468 \times 10^{-10} \pm 3.933 \times 10^{-12}$	$5.993 \times 10^{-11} \pm 1.287 \times 10^{-11}$	$-5.685 \times 10^{-11} \pm 4.300 \times 10^{-11}$	$2.582 \times 10^{-10} \pm 3.353 \times 10^{-11}$	$-2.941 \times 10^{-10} \pm 7.556 \times 10^{-11}$	2.033
353.15	$-1.554 \times 10^{-10} \pm 4.463 \times 10^{-12}$	$6.038 \times 10^{-11} \pm 1.460 \times 10^{-11}$	$-6.589 \times 10^{-11} \pm 4.879 \times 10^{-11}$	$2.798 \times 10^{-10} \pm 3.805 \times 10^{-11}$	$-2.977 \times 10^{-10} \pm 8.574 \times 10^{-11}$	2.618

**Table 10.** Intermolecular Free Length ( $L_f/m$ ) of ChCl/AcA DES–DMSO Mixtures as a Function of Mole Fraction ( $x_1$ )<sup>a</sup>

$x_1/T$ (K)	$L_f \times 10^{11}/m$											
	298.15	303.15	308.15	313.15	318.15	323.15	328.15	333.15	338.15	343.15	348.15	353.15
0.00	4.076	4.171	4.270	4.370	4.474	4.578	4.685	4.796	4.908	5.024	5.142	5.264
0.10	3.907	3.992	4.080	4.169	4.261	4.355	4.451	4.549	4.649	4.752	4.856	4.965
0.20	3.849	3.931	4.015	4.101	4.189	4.280	4.372	4.466	4.563	4.662	4.762	4.865
0.30	3.793	3.874	3.956	4.039	4.125	4.213	4.303	4.394	4.489	4.585	4.680	4.780
0.40	3.761	3.839	3.919	4.001	4.084	4.170	4.258	4.347	4.438	4.531	4.625	4.722
0.50	3.720	3.796	3.873	3.951	4.031	4.112	4.196	4.280	4.364	4.451	4.535	4.626
0.60	3.685	3.759	3.834	3.911	3.989	4.069	4.149	4.229	4.308	4.388	4.476	4.565
0.70	3.637	3.708	3.780	3.854	3.928	4.004	4.082	4.161	4.242	4.324	4.407	4.488
0.80	3.607	3.675	3.746	3.818	3.891	3.964	4.040	4.118	4.197	4.277	4.358	4.441
0.90	3.578	3.644	3.711	3.780	3.851	3.922	3.994	4.068	4.143	4.220	4.299	4.378
1.00	3.557	3.622	3.688	3.755	3.824	3.894	3.964	4.037	4.110	4.185	4.261	4.338

<sup>a</sup>Standard uncertainties ( $u$ ) in  $T$ ,  $x$ ,  $P$ , and  $u$  are  $u(T) = 0.01$  K,  $u(x_1) = 0.01$ ,  $u(P) = 10$  kPa, and  $u_r(u) = 0.5$ .

the DES concentration is increased. The increase in  $L_f$  on increasing temperature is due to thermal agitation in the liquid mixture resulting in more free space in DES.<sup>55</sup> The variation of  $L_f$  with the temperature and DES concentration reinforces the results concluded from  $\kappa_S^E$  in terms of intermolecular interactions.

Acoustic impedance ( $Z$ ) is the physical property that describes the resistance faced by an ultrasound beam while passing through the medium.<sup>74</sup> The value of  $Z$  is calculated by eq 13.

$$Z = \rho \cdot u \quad (13)$$

where  $\rho$  (kg m<sup>-3</sup>) is density and  $u$  (m s<sup>-1</sup>) is the speed of sound. The calculated values of  $Z$  (eq 13) are listed in Table 11 and plotted in Figure 7.

The dependence of  $Z$  and  $L_f$  parameters on DES concentration and temperature is reversed. The value of  $Z$  increases with increasing concentration of DES at all temperatures, indicating strong interactions among components of the liquid mixture.<sup>71,75</sup>

**3.3. Viscosity.** The knowledge of viscosity ( $\eta$ ) an important transport property of fluids is desirable because of its practical applications in designing process equipment, mass transfer, and reaction rate calculations.<sup>76</sup> Factors that influence  $\eta$  of DESs are temperature, mole ratio, water content and molecular weight.<sup>77</sup> Because most DESs are relatively more viscous than conventional organic solvents, it becomes necessary that their mixtures with molecular liquids (e.g., water, DMSO, alcohols) should be used in industrial processes.<sup>78</sup>

In this study, the dynamic viscosity of ChCl/AcA DES and its binary mixtures with DMSO is measured in the 298.15 to 353.15 K range, and the values are reported in Table 12. Figure 8 shows the plot of  $\ln \eta$  against  $T$ .

Table 12 shows that viscosity of the mixture increases with DES mole fraction at all temperatures, but it decreases as the temperature is increased for all compositions.<sup>79</sup>

The Vogel–Fulcher–Tammann (VFT) model (eq 14) is applied to investigate the temperature dependence of transport

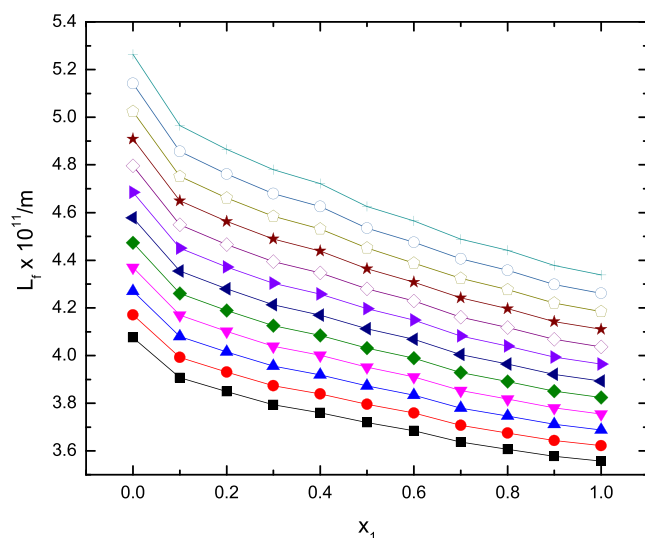


**Figure 6.** Intermolecular free length ( $L_f \times 10^{11}/m$ ) of ChCl/AcA DES–DMSO mixtures as a function of  $x_1$  in the temperature range  $298.15 \leq T/K \leq 353.15$  (■(black)): 298.15 K; ●(red): 303.15 K; ▲(blue): 308.15 K; ▼(magenta): 313.15 K; ◆(olive): 318.15 K; ◀(navy): 323.15 K; ▶(violet): 328.15 K; ◇(purple): 333.15 K; ★(wine): 338.15 K; ◇(dark yellow): 343.15 K; ○(grey blue): 348.15 K; +(teal) : 353.15 K.

property,  $Y$ , of viscous liquids close to their glass transition temperature.<sup>26,80</sup>

$$\ln\left(\frac{Y}{Y^0}\right) = \ln\left(\frac{A_Y}{Y^0}\right) + \frac{B_Y}{(T - T_{0,Y})} \quad (14)$$

where  $Y$  is viscosity  $\eta$  ( $Y^0 = \eta^0 = 1 \text{ mPa}^{-1}$ ) or resistivity  $K^{-1}$  ( $Y^0 = \frac{1}{\kappa^0} = 1 \text{ S}^{-1} \text{ m}$ ) and  $A_Y$ ,  $B_Y$ , and  $T_{0,Y}$  are adjustable parameters. The experimental data obtained at various temperatures are fitted with eq 14 by adjusting the VFT parameters.<sup>81</sup> The VFT equation explains that the system's dynamics is slowed down on approaching the critical VFT (or Vogel) temperature,  $T_{0,Y}$ , which is usually 10–15 K below the calorimetric glass transition temperature of the system.  $A_Y$  represents the property  $Y$  (viscosity or resistivity) as  $T \rightarrow \infty$ , the quantity  $E_a = B_Y \times R$  (where  $R$  is a general gas constant) is the pseudo activation energy, and  $T_{0,Y}$  is the Vogel temper-

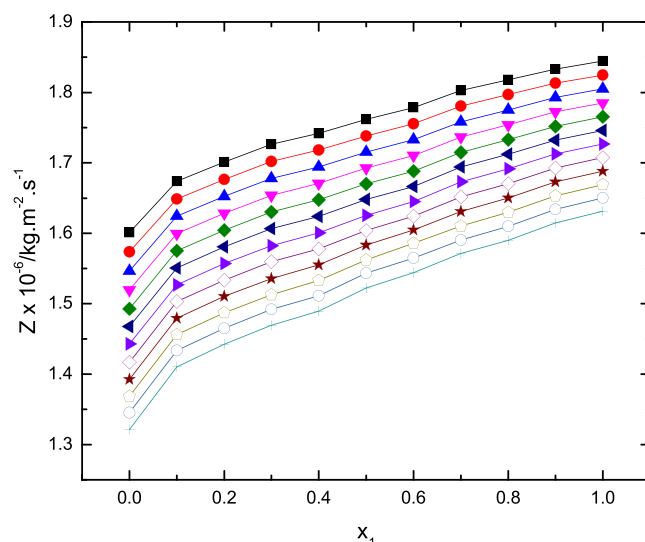


**Figure 7.** Acoustic impedance ( $Z \times 10^{-6}/\text{kg m}^{-2} \text{ s}^{-1}$ ) of ChCl/AcA DES–DMSO mixtures as a function of  $x_1$  in the temperature range  $298.15 \leq T/K \leq 353.15$  (■(black)): 298.15 K; ●(red): 303.15 K; ▲(blue): 308.15 K; ▼(magenta): 313.15 K; ◆(olive): 318.15 K; ◀(navy): 323.15 K; ▶(violet): 328.15 K; ◇(purple): 333.15 K; ★(wine): 338.15 K; ◇(dark yellow): 343.15 K; ○(grey blue): 348.15 K; +(teal) : 353.15 K.

ature. The calculated values of these fitting parameters are listed in Table 13.

The solid lines are the best fit representation of eq 14.

The Arrhenius equation is also used to correlate the temperature dependence of viscosity ( $\eta$ ) and electrical conductivity ( $\kappa$ ) of ChCl/AcA DES and its binary mixtures with DMSO. The calculated parameters are shown in Tables S11 and S12 and plotted as a function of  $1/T$  in Figures S7 and S8, respectively (Supporting Information).

The viscosity deviation,  $\Delta\eta$ , is calculated from eq 15 for the viscous fluids.

$$\Delta\eta = \eta - \sum_i x_i \eta_i \quad (15)$$

where  $x_i$  and  $\eta_i$  are mole fractions and dynamic viscosity of component  $i$ , respectively. Calculated values of  $\Delta\eta$  are collected in Table 14, and its plot as a function of  $x_1$  is shown in Figure 9 for all temperatures investigated.

**Table 11. Acoustic Impedance ( $Z/\text{kg m}^{-2} \text{ s}^{-1}$ ) of ChCl/AcA DES–DMSO Mixtures as a Function of Mole Fraction ( $x_1$ )<sup>a</sup>**

$x_1/T$ (K)	$Z \times 10^{-6}/\text{kg m}^{-2} \text{ s}^{-1}$											
	298.15	303.15	308.15	313.15	318.15	323.15	328.15	333.15	338.15	343.15	348.15	353.15
0.00	1.601	1.574	1.546	1.520	1.493	1.468	1.443	1.417	1.393	1.369	1.345	1.321
0.10	1.674	1.649	1.624	1.600	1.575	1.551	1.527	1.503	1.480	1.456	1.434	1.410
0.20	1.701	1.677	1.652	1.628	1.604	1.581	1.557	1.534	1.510	1.487	1.465	1.442
0.30	1.726	1.702	1.678	1.654	1.630	1.606	1.582	1.560	1.536	1.513	1.492	1.470
0.40	1.742	1.718	1.694	1.671	1.647	1.624	1.601	1.578	1.555	1.533	1.511	1.489
0.50	1.762	1.738	1.715	1.693	1.670	1.648	1.625	1.604	1.583	1.562	1.543	1.522
0.60	1.779	1.755	1.733	1.711	1.688	1.667	1.645	1.624	1.605	1.586	1.565	1.544
0.70	1.803	1.780	1.758	1.737	1.715	1.694	1.673	1.652	1.631	1.610	1.590	1.572
0.80	1.818	1.797	1.775	1.754	1.733	1.712	1.691	1.671	1.650	1.630	1.610	1.590
0.90	1.833	1.813	1.793	1.772	1.752	1.732	1.713	1.693	1.673	1.653	1.634	1.615
1.00	1.845	1.825	1.805	1.785	1.765	1.746	1.727	1.707	1.688	1.669	1.650	1.631

<sup>a</sup>Standard uncertainties ( $u$ ) in  $T$ ,  $x$ ,  $P$ , and  $u$  are  $u(T) = 0.01 \text{ K}$ ,  $u(x_1) = 0.01$ ,  $u(P) = 10 \text{ kPa}$ , and  $u_r(u) = 0.5$ .

**Table 12.** Dynamic Viscosity ( $\eta$ /mPa s) of ChCl/AcA DES–DMSO Mixtures as a Function of Temperature  $T = 298.15$  to  $353.15$  K and Pressure  $p = 0.1$  MPa<sup>a</sup>

$x_1/T$ (K)	$\eta$ /mPa s											
	298.15	303.15	308.15	313.15	318.15	323.15	328.15	333.15	338.15	343.15	348.15	353.15
0.00	1.856	1.751	1.650	1.510	1.390	1.280	1.190	1.110	1.030	0.948	0.901	0.857
0.10	3.030	2.707	2.433	2.198	1.997	1.820	1.674	1.544	1.433	1.336	1.244	1.141
0.20	4.119	3.637	3.237	2.895	2.609	2.365	2.154	1.970	1.805	1.660	1.533	1.406
0.30	4.596	4.123	3.696	3.339	3.038	2.779	2.557	2.366	2.199	2.053	1.924	1.806
0.40	5.228	4.693	4.260	3.886	3.589	3.286	3.025	2.829	2.642	2.456	2.323	2.220
0.50	8.476	7.067	6.075	5.127	4.503	3.985	3.633	3.374	3.190	2.956	2.850	2.726
0.60	13.00	11.03	9.150	7.420	6.235	5.243	4.579	4.080	3.776	3.512	3.299	3.180
0.70	17.34	14.52	12.13	10.17	8.646	7.296	6.149	5.352	4.740	4.309	3.889	3.704
0.80	27.57	22.06	18.64	16.01	13.37	10.82	9.231	7.607	6.404	5.605	4.964	4.485
0.90	42.86	34.13	28.76	23.70	20.01	17.24	14.32	12.10	10.33	8.930	7.773	6.900
1.00	57.88	46.62	39.79	33.14	27.64	23.89	20.26	17.93	15.89	13.98	12.59	11.59

<sup>a</sup>Standard uncertainties ( $u$ ) in  $T$ ,  $x$ ,  $P$ , and  $\eta$  are  $u(T) = 0.01$  K,  $u(x_1) = 0.01$ ,  $u(P) = 10$  kPa, and  $u_r(\eta) = 0.01$ .

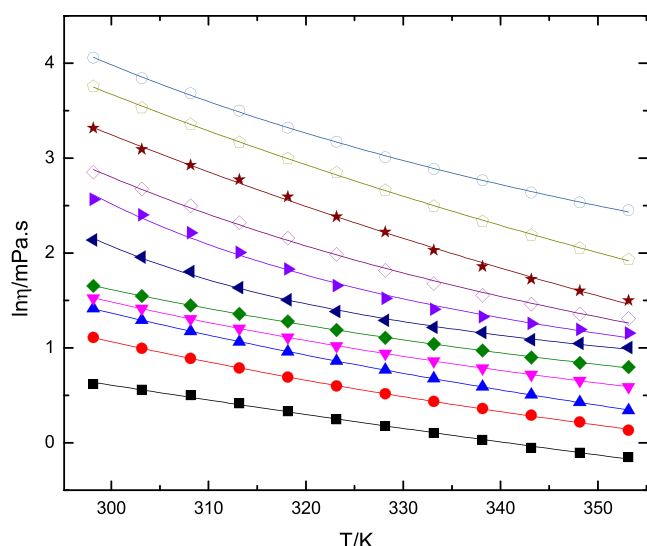


**Figure 8.** Temperature and composition dependence of viscosity  $\eta$  for pure ChCl/AcA DES, DMSO, and their binary mixtures measured at atmospheric pressure;  $x_1$  = (■)(black): 0.0; (●)(red): 0.1; (▲)(blue): 0.2; (▼)(magenta): 0.3; (◆)(olive): 0.4; (◀)(navy): 0.5; (▶)(violet): 0.6; (◇)(purple): 0.7; (★)(wine): 0.8; (◇)(dark yellow): 0.9; (○)(grey blue): 1.00).

**Table 13.** VFT Parameters from Eq 14 for Dynamic Viscosity  $\eta$  and Associated Standard Deviations:  $\eta^0 = 1$  mPa s

$x_1$	$\ln\left(\frac{A_\eta}{\eta^0}\right)$	$B_\eta/K$	$T_{0,\eta}/K$
0.00	$-8.886 \pm 5.682$	$5642.7 \pm 7030.4$	$-294.35 \pm 384.18$
0.10	$-2.889 \pm 0.235$	$691.4 \pm 93.21$	$125.15 \pm 13.22$
0.20	$-3.384 \pm 0.177$	$924.08 \pm 77.14$	$105.51 \pm 9.027$
0.30	$-1.734 \pm 0.054$	$445.23 \pm 17.38$	$161.72 \pm 3.095$
0.40	$-1.380 \pm 0.158$	$417.83 \pm 51.54$	$160.46 \pm 9.860$
0.50	$0.001 \pm 0.094$	$99.65 \pm 12.67$	$251.87 \pm 3.971$
0.60	$-0.487 \pm 0.298$	$180.49 \pm 47.60$	$239.95 \pm 9.997$
0.70	$-1.930 \pm 0.550$	$522.41 \pm 145.73$	$189.56 \pm 18.08$
0.80	$-6.900 \pm 2.414$	$2525.9 \pm 1317.3$	$51.06 \pm 70.86$
0.90	$-6.124 \pm 1.033$	$2385.6 \pm 552.54$	$56.50 \pm 30.82$
1.00	$-1.103 \pm 0.304$	$616.39 \pm 87.25$	$178.84 \pm 9.966$

The  $\Delta\eta$  values are negative for all compositions and temperatures and reflect the strength of interaction between components of the mixture.<sup>82,83</sup>

Negative  $\Delta\eta$  values are associated with differences in shape and size of the component molecules and loss of dipolar association, whereas specific interactions such as H-bonding and charge transfer complex formation led to positive contribution to  $\Delta\eta$ .<sup>76</sup>

Figure 9 shows that a minimum occurs at about  $x_1 \approx 0.62$ , which lies in the region rich in DES. With increasing DES content, interaction forces are progressively weakening up to the minimum limit. The behavior is more prominent at lower temperatures, which could be correlated with the size and shapes of the component molecules. At  $x_1 > 0.62$ , absolute values of  $\Delta\eta$  decrease, which indicate the dominance of specific forces in the system. Negative  $\Delta\eta$  values support the presence of a weak interaction between DES and DMSO molecules and the breaking of self-associated structures of DMSO molecules. The calculated parameters from the Redlich–Kister equation for  $\Delta\eta$  are listed in Table 15.

**3.4. Electrical Conductivity.** Knowledge of electrical conductivity and  $\kappa$  of DESs is required for their industrial applications in the design, control, and optimization of electrochemical processes. DESs, which are usually highly viscous fluids, exhibit low ionic conductivity ( $\kappa < 2$  mS cm<sup>-1</sup> at room temperature).<sup>84,85</sup> The  $\kappa$  increases with an increase in temperature due to the resulting decrease in viscosity. In a less viscous medium, the mobility of charged molecular species increases.

The  $\kappa$  of ChCl/AcA DES and its binary mixtures with DMSO was measured in the  $T = 298.15$  to  $353.15$  K range over the entire composition range. Experimentally measured  $\kappa$  values are reported in Table 16, and the plots of  $\ln \kappa^{-1}$  vs  $T$  and  $\kappa$  vs  $x_1$  are shown in Figures 10 and 11, respectively.

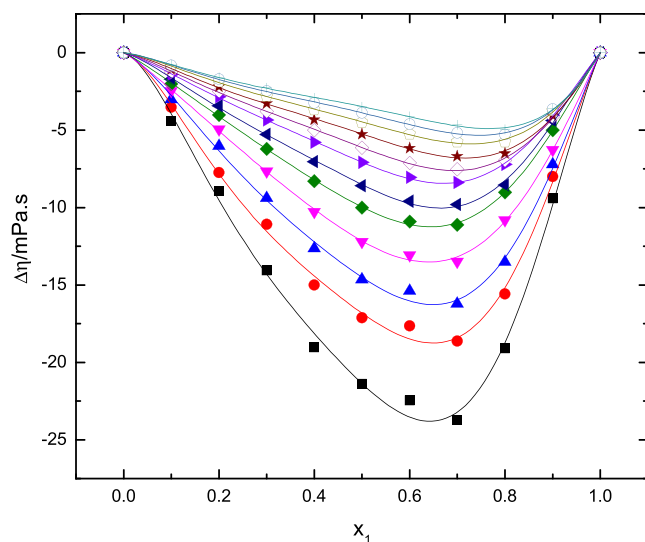
The solid lines are the best fit representation of eq 14.

Table 16 shows that  $\kappa$  has increased with the increase in temperature for all compositions, which is attributed to the decrease in viscosity (Table 12).  $\kappa$  of the DES increased with increase in DES content in the mixture, which is in opposition to the observed increase in viscosity. The increase in conductivity following an increase in temperature is due to the greater mobility of charges as a result of the weakening of intermolecular forces. The concentration effect could be due to the increase in the number of charge species. The experimental

**Table 14.** Viscosity Deviation  $\Delta\eta$  of ChCl/AcA DES–DMSO Binary Mixtures as a Function of ChCl/AcA DES Mole Fraction  $x_1$  in the Temperature Range  $298.15 \leq T/K \leq 353.15^a$ 

$x_1/T$ (K)	$\Delta\eta/mPa\ s$											
	298.15	303.15	308.15	313.15	318.15	323.15	328.15	333.15	338.15	343.15	348.15	353.15
0.00	0	0	0	0	0	0	0	0	0	0	0	0
0.10	-4.428	-3.531	-3.031	-2.475	-2.018	-1.721	-1.423	-1.248	-1.083	-0.915	-0.826	-0.789
0.20	-8.942	-7.748	-6.041	-4.941	-4.031	-3.437	-2.850	-2.504	-2.197	-1.894	-1.706	-1.598
0.30	-14.07	-11.09	-9.396	-7.660	-6.227	-5.284	-4.354	-3.790	-3.289	-2.804	-2.483	-2.271
0.40	-19.04	-15.01	-12.65	-10.28	-8.301	-7.038	-5.793	-5.009	-4.333	-3.705	-3.253	-2.931
0.50	-21.39	-17.12	-14.65	-12.20	-10.01	-8.600	-7.092	-6.146	-5.271	-4.508	-3.895	-3.499
0.60	-22.47	-17.64	-15.38	-13.07	-10.91	-9.603	-8.053	-7.122	-6.171	-5.255	-4.614	-4.118
0.70	-23.73	-18.64	-16.21	-13.48	-11.12	-9.811	-8.391	-7.533	-6.693	-5.761	-5.193	-4.668
0.80	-19.11	-15.59	-13.52	-10.80	-9.020	-8.548	-7.216	-6.960	-6.515	-5.769	-5.287	-4.960
0.90	-9.418	-8.003	-7.216	-6.277	-5.005	-4.389	-4.034	-4.149	-4.080	-3.746	-3.648	-3.618
1	0	0	0	0	0	0	0	0	0	0	0	0

<sup>a</sup>Standard uncertainties ( $u$ ) in  $T$ ,  $x$ ,  $P$ , and  $\eta$  are  $u(T) = 0.01$  K,  $u(x_1) = 0.01$ ,  $u(P) = 10$  kPa, and  $u_r(\eta) = 0.01$ .



**Figure 9.** Viscosity deviation  $\Delta\eta$  of ChCl/AcA DES–DMSO binary mixtures as a function of  $x_1$  in the temperature range  $298.15 \leq T/K \leq 353.15$  (■(black): 298.15 K; ●(red): 303.15 K; ▲(blue): 308.15 K; ▼(magenta): 313.15 K; ◆(olive): 318.15 K; ▲(navy): 323.15 K; ▶(violet): 328.15 K; ◇(purple): 333.15 K; ★(wine): 338.15 K; △(dark yellow): 343.15 K; ○(grey blue): 348.15 K; +(teal): 353.15 K).

$\kappa$  data were fitted with the VFT eq 14, and the calculated fitting parameter are listed in Table 17.

The  $B_\kappa$  and  $T_{0,\kappa}$  values in Table 16 show considerable scattering as with the corresponding values obtained for the viscosity data.

The dependence of  $\kappa$  on the composition of the mixture is explained by empirical Casteel–Amis eq 16.<sup>46,86,87</sup>

$$\kappa = \kappa_{\max} \left( \frac{x_{\text{DES}}}{x_{\max}} \right)^a \exp \left[ b(x_{\text{DES}} - x_{\max})^2 - a \frac{x_{\text{DES}} - x_{\max}}{x_{\max}} \right] \quad (16)$$

where  $x_{\max}$  is the mole fraction of DES at  $\kappa_{\max}$  the maximum conductivity, and  $a$  and  $b$  are adjustable parameters without any specific meanings. Figure 11 shows that conductivity increases exponentially with an increase in mole fraction of DES particularly at higher temperatures. The resulting fitting parameters of eq 16 are listed in Table 18.

The solid lines are the best fit representations of eq 16.

The correlation between conductivity and viscosity is explained in terms of the (1) reduction in the number of charge carriers due to aggregate formation and (2) reduced mobility of charge carriers due to high viscosity. The former effect is the major factor for the variation of  $\kappa$ .<sup>88,89</sup>

#### 4. CONCLUSIONS

Choline chloride is a bifunctional quaternary ammonium salt consisting of choline cation and chloride as counterion.

**Table 15.** Fit parameters ( $A_j$ ) of the Redlich–Kister Equation (Eq 5) for Viscosity Deviation  $\Delta\eta$  of ChCl/AcA DES–DMSO Mixtures

T/K	$A_0$	$A_1$	$A_2$	$A_3$	$A_4$	$\sigma$
298.15	$-85.46 \pm 1.991$	$-57.17 \pm 6.518$	$-36.66 \pm 21.77$	$25.81 \pm 16.97$	$79.36 \pm 38.25$	0.521
303.15	$-67.30 \pm 1.476$	$-42.88 \pm 4.833$	$-34.41 \pm 16.14$	$12.89 \pm 12.59$	$59.74 \pm 28.36$	0.287
308.15	$-58.02 \pm 1.129$	$-40.23 \pm 3.696$	$-22.82 \pm 12.34$	$11.98 \pm 9.628$	$38.42 \pm 21.69$	0.168
313.15	$-48.64 \pm 0.569$	$-34.59 \pm 1.863$	$-8.821 \pm 6.224$	$11.73 \pm 4.853$	$14.98 \pm 10.93$	0.043
318.15	$-39.88 \pm 0.318$	$-30.62 \pm 1.043$	$-9.727 \pm 3.487$	$14.32 \pm 2.719$	$17.78 \pm 6.127$	0.013
323.15	$-34.07 \pm 0.477$	$-29.87 \pm 1.561$	$-18.04 \pm 5.216$	$14.86 \pm 4.067$	$27.65 \pm 9.165$	0.030
328.15	$-28.29 \pm 0.208$	$-25.66 \pm 0.683$	$-15.91 \pm 2.282$	$10.48 \pm 1.779$	$19.89 \pm 4.010$	0.006
333.15	$-24.50 \pm 0.253$	$-23.24 \pm 0.830$	$-19.20 \pm 2.774$	$3.311 \pm 2.163$	$16.18 \pm 4.874$	0.008
338.15	$-20.99 \pm 0.294$	$-20.32 \pm 0.962$	$-21.38 \pm 3.215$	$-2.467 \pm 2.507$	$14.01 \pm 5.649$	0.011
343.15	$-17.88 \pm 0.276$	$-17.09 \pm 0.904$	$-19.23 \pm 3.022$	$-5.503 \pm 2.357$	$9.764 \pm 5.311$	0.010
348.15	$-15.55 \pm 0.186$	$-14.92 \pm 0.611$	$-19.45 \pm 2.042$	$-8.345 \pm 1.592$	$7.297 \pm 3.589$	0.005
353.15	$-13.91 \pm 0.178$	$-12.57 \pm 0.585$	$-18.15 \pm 1.956$	$-11.92 \pm 1.525$	$2.024 \pm 3.437$	0.004

**Table 16.** Electrical Conductivity ( $\kappa/S\text{ m}^{-1}$ ) of ChCl/AcA DES–DMSO Mixtures as a Function of Temperature  $T = 298.15$  to  $353.15\text{ K}$  and Pressure  $p = 0.1\text{ MPa}^a$ 

$x_1/T\text{ (K)}$	$\kappa/S\text{ m}^{-1}$											
	298.15	303.15	308.15	313.15	318.15	323.15	328.15	333.15	338.15	343.15	348.15	353.15
0.10	0.552	0.573	0.591	0.606	0.623	0.644	0.663	0.687	0.716	0.738	0.762	0.789
0.20	0.849	0.874	0.897	0.926	0.950	0.978	1.011	1.051	1.084	1.127	1.156	1.197
0.30	1.004	1.045	1.079	1.123	1.152	1.198	1.249	1.301	1.357	1.421	1.478	1.538
0.40	1.123	1.178	1.216	1.267	1.317	1.372	1.429	1.500	1.567	1.672	1.737	1.822
0.50	1.230	1.281	1.358	1.405	1.452	1.523	1.603	1.689	1.758	1.876	1.938	2.047
0.60	1.318	1.382	1.448	1.534	1.599	1.691	1.784	1.844	1.968	2.099	2.242	2.357
0.70	1.338	1.417	1.484	1.600	1.669	1.792	1.886	2.026	2.135	2.324	2.484	2.661
0.80	1.427	1.524	1.609	1.688	1.773	1.893	2.010	2.137	2.312	2.473	2.664	2.776
0.90	1.516	1.575	1.706	1.802	1.912	2.053	2.212	2.359	2.535	2.699	2.884	3.122
1.00	1.666	1.771	1.847	1.939	2.080	2.219	2.383	2.527	2.712	2.890	3.053	3.253

<sup>a</sup>Standard uncertainties ( $u$ ) in  $T$ ,  $x$ ,  $p$ , and  $\kappa$  are  $u(T) = 0.01\text{ K}$ ,  $u(x_1) = 0.01$ ,  $u(P) = 10\text{ kPa}$ , and  $u_r(\kappa) = 0.005$ .

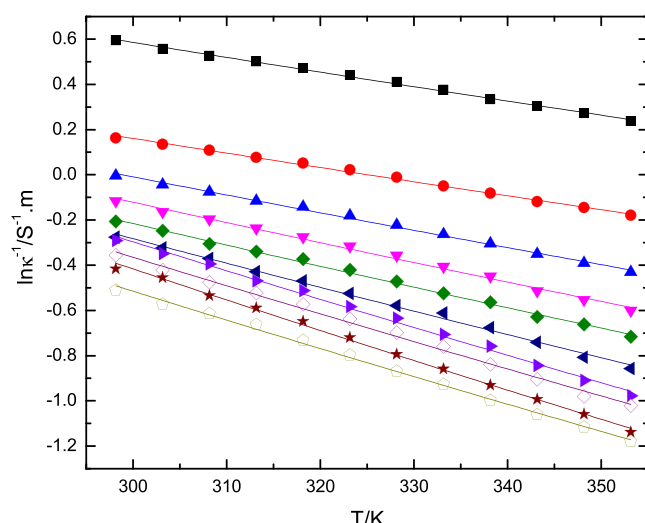


**Figure 10.** Temperature and composition dependence of the electrical conductivity  $\kappa$  of pure ChCl/AcA DES and its binary mixtures with DMSO;  $x_1$  = (■(black)): 0.1; ●(red): 0.2; ▲(blue): 0.3; ▼(magenta): 0.4; ◆(olive): 0.5; ▲(navy): 0.6; ▷(violet): 0.7; ◇(purple): 0.8; ★(wine): 0.9; ◇(dark yellow): 1.0.

Choline cation occurs in nature. Choline chloride is a major industrial product with a market value of 662.1 million US dollars in 2022 that is projected to increase further in future. Acetic acid is a byproduct of fermentation. The present study reports the preparation of ChCl/AcA DES using choline chloride and acetic acid and investigation of its physicochemical properties along with its binary mixtures with DMSO in the temperature range  $T = 298.15$  to  $353.15\text{ K}$  for all compositions. The regression analysis of experimental density data is fitted with a second-degree polynomial in  $T$ . The statistical  $r^2$  values of the fit are collected in Table 3, which shows the goodness of the fit and success of the model. Excess properties ( $V^E$ ,  $\kappa_S^E$ , and  $\Delta\eta$ ) calculated from the respective properties of the pure DES and its binary mixtures with DMSO for all temperatures and compositions are fitted with the Redlich–Kister polynomial equation. The negative values of  $V^E$  are attributed to the presence of specific interactions or the packing effect between components of the mixture. The minima in the  $V^E$  vs  $x_1$  curves lie in the DMSO-rich region at  $x_1 \approx 0.15$ , which indicates stronger interaction between the components of the mixture at this composition. This behavior

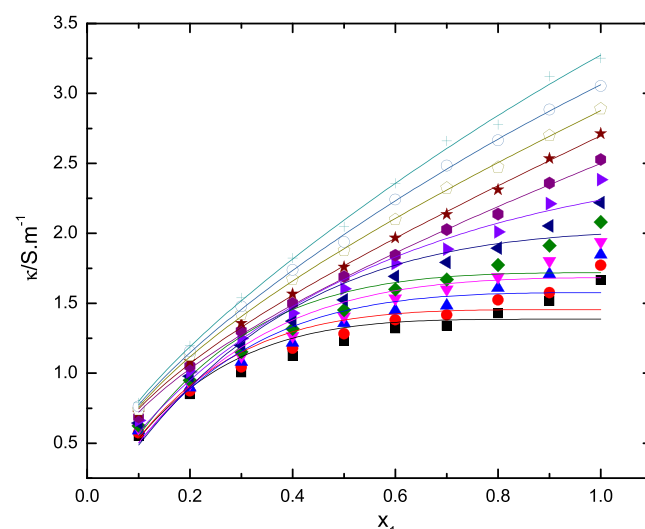


**Figure 11.** Variation of electrical conductivity  $\kappa$  of ChCl/AcA DES–DMSO mixtures with mole fraction of ChCl/AcA DES  $x_1$  in the temperature range  $283.15 \leq T/\text{K} \leq 353.15$  (■(black)): 298.15 K; ●(red): 303.15 K; ▲(blue): 308.15 K; ▼(magenta): 313.15 K; ◆(olive): 318.15 K; ▲(navy): 323.15 K; ▷(violet): 328.15 K; ◇(purple): 333.15 K; ★(wine): 338.15 K; ◇(dark yellow): 343.15 K; ○(grey blue): 348.15 K; + (teal): 353.15 K.

**Table 17.** VFT Parameters of Eq 14 for Electrical Conductivity  $\kappa$  and Associated Standard Deviations:  $\kappa^0 = 1\text{ S m}^{-1}$

$x_1$	$\ln(A\kappa \times \kappa^0)$	$B_\kappa/\text{K}$	$T_{0,\kappa}/\text{K}$
0.10	$-8.149 \pm 13.34$	$11422 \pm 35504$	$-1007.6 \pm 2059.6$
0.20	$-8.675 \pm 14.72$	$11946 \pm 40498$	$-1052.1 \pm 2320.9$
0.30	$-11.14 \pm 19.92$	$15424 \pm 56094$	$-1084.7 \pm 2548.9$
0.40	$-13.26 \pm 29.11$	$19017 \pm 85591$	$-1147.4 \pm 3294.5$
0.50	$-12.59 \pm 20.06$	$15961 \pm 52645$	$-988.95 \pm 2154.9$
0.60	$-15.32 \pm 28.94$	$20737 \pm 81091$	$-1078.1 \pm 2727.9$
0.70	$-18.35 \pm 34.58$	$25250 \pm 98296$	$-1098.4 \pm 2755.1$
0.80	$-18.14 \pm 36.81$	$24859 \pm 104640$	$-1098.5 \pm 2979.1$
0.90	$-17.98 \pm 23.22$	$22327 \pm 60097$	$-970.86 \pm 1734.3$
1.00	$-16.90 \pm 24.10$	$20841 \pm 62407$	$-971.46 \pm 1930.3$

can be explained by considering the structure of DMSO in the liquid state and in solutions. The presence of dimeric and/or larger associations among DMSO molecules in the pure liquid state and in solutions is known. At higher mole fractions of

**Table 18. Fit Parameters ( $\kappa_{\max}$ ,  $x_{\max}$ ,  $a$ , and  $b$ ) of the Casteel–Amis Equation (Eq 16) for the Electrical Conductivity ( $\kappa$ ) of ChCl/AcA DES–DMSO Mixtures**

temperature T/K	$\kappa_{\max}$ (S m <sup>-1</sup> )	$a$	$b$	$x_{\max}$	$\sigma$
298.15	1.482	1.057	0.668	0.888	$2.3 \times 10^{-2}$
303.15	1.453	1.072	0.636	0.917	$2.6 \times 10^{-2}$
308.15	1.576	1.113	0.515	1.037	$2.2 \times 10^{-2}$
313.15	1.684	1.109	0.442	1.117	$2.0 \times 10^{-2}$
318.15	1.717	1.101	0.507	1.038	$3.8 \times 10^{-2}$
323.15	2.018	1.101	0.272	1.419	$2.0 \times 10^{-2}$
328.15	2.523	0.807	0.060	2.579	$8.8 \times 10^{-3}$
333.15	74.03	0.499	-0.002	37.10	$1.1 \times 10^{-3}$
338.15	89.37	0.496	-0.003	27.75	$6.2 \times 10^{-4}$
343.15	24.92	0.547	-0.003	20.33	$4.3 \times 10^{-4}$
348.15	4.166	0.526	-0.129	2.187	$7.4 \times 10^{-3}$
353.15	4.483	0.524	-0.146	2.148	$2.3 \times 10^{-3}$

DMSO, DES molecules are trapped in the DMSO clusters producing a compact structure in the mixed state. With increasing concentration of the DES, these clusters break, and the compact structure is progressively demolished. The negative  $\Delta\eta$  values are smaller in magnitude than observed for  $V^E$ , and the minima in the  $\Delta\eta$  vs  $x_1$  curves also shift to  $x_1 \approx 0.62$  in the region of higher DES concentration. These results show the progressive domination of weak interactions in the mixture and the breaking of self-associated structures of DMSO molecules. The observed  $\kappa_s^E$  values are also negative, exhibiting a minimum located at  $x_1 \approx 0.15$  in the  $\kappa_s^E$  vs  $x_1$  plots. The Vogel–Fulcher–Tammann (VFT) model is reasonably applicable to variation of the transport properties ( $\eta$  and  $\kappa$ ) with temperature compared to the Arrhenius model. The behavior observed in the variation of electrical conductivity  $\kappa$  with temperature is highlighted with the Casteel–Amis equation.

## ASSOCIATED CONTENT

### Supporting Information

The Supporting Information is available free of charge at <https://pubs.acs.org/doi/10.1021/acsomega.3c07739>.

FTIR and <sup>1</sup>H spectra of ChCl/AcA DES; spectral profile of ChCl/AcA DES, DMSO, and their binary mixtures; apparent and excess partial molar volumes of ChCl/AcA DES and DMSO; and Arrhenius equation (viscosity and electrical conductivity) (PDF)

## AUTHOR INFORMATION

### Corresponding Author

Athar Yaseen Khan – Department of Chemistry, Forman Christian College (A Chartered University), Lahore 54600, Pakistan; [orcid.org/0000-0002-8813-5035](https://orcid.org/0000-0002-8813-5035); Email: [atharkhan@fccollege.edu.pk](mailto:atharkhan@fccollege.edu.pk)

### Authors

Aafia Sheikh – Department of Chemistry, Government College Women University, Sialkot 51310, Pakistan; Department of Chemistry, Forman Christian College (A Chartered University), Lahore 54600, Pakistan; [orcid.org/0000-0001-5861-4425](https://orcid.org/0000-0001-5861-4425)

Safeer Ahmed – Department of Chemistry, Quaid-i-Azam University, Islamabad 45320, Pakistan; [orcid.org/0000-0003-0074-2517](https://orcid.org/0000-0003-0074-2517)

Complete contact information is available at: <https://pubs.acs.org/10.1021/acsomega.3c07739>

## Notes

The authors declare no competing financial interest.

## ACKNOWLEDGMENTS

The authors are thankful to the Department of Physics, Forman Christian College, A Chartered University, Lahore, Pakistan, and the Department of Chemistry, Quaid-i-Azam University, Islamabad, Pakistan, for providing technical support.

## REFERENCES

- Abbott, A. P.; Capper, G.; Davies, D. L.; Munro, H. L.; Rasheed, R. K.; Tambyrajah, V. Preparation of novel, moisture-stable, Lewis-acidic ionic liquids containing quaternary ammonium salts with functional side chains. *Chem. Commun.* **2001**, *19*, 2010–2011.
- Abbott, A. P.; Capper, G.; Davies, D. L.; Rasheed, R. K.; Tambyrajah, V. Novel solvent properties of choline chloride/urea mixtures. *Chem. Commun.* **2003**, *1*, 70–71.
- Abbott, A. P.; Boothby, D.; Capper, G.; Davies, D. L.; Rasheed, R. K. Deep eutectic solvents formed between choline chloride and carboxylic acids: versatile alternatives to ionic liquids. *J. Am. Chem. Soc.* **2004**, *126*, 9142–9147.
- Shaibuna, M.; Theresa, L. V.; Sreekumar, K. Neoteric deep eutectic solvents: history, recent developments, and catalytic applications. *Soft Matter* **2022**, *18*, 2695–2721.
- Smith, E. L.; Abbott, A. P.; Ryder, K. S. Deep eutectic solvents (DESs) and their applications. *Chem. Rev.* **2014**, *114*, 11060–11082.
- Paiva, A.; Craveiro, R.; Aroso, I.; Martins, M.; Reis, R. L.; Duarte, A. R. C. Natural deep eutectic solvents - Solvents for the 21st Century. *ACS Sustainable Chem. Eng.* **2014**, *2*, 1063–1071.
- Boldrini, C. L.; Manfredi, N.; Perna, F. M.; Trifiletti, V.; Capriati, V.; Abbotto, A. Dye-sensitized solar cells that use an aqueous choline chloride-based deep eutectic solvent as effective electrolyte solution. *Energy Technol.* **2017**, *5*, 345–353.
- Zhang, C.; Ding, Y.; Zhang, L.; Wang, X.; Zhao, Y.; Zhang, X.; Yu, G. A sustainable redox-flow battery with an aluminum-based, deep-eutectic-solvent anolyte. *Angew. Chem.* **2017**, *129*, 7562–7567.
- Lloyd, D.; Vainikka, T.; Kontturi, K. The development of an all-copper hybrid redox flow battery using deep eutectic solvents. *Electrochim. Acta* **2013**, *100*, 18–23.
- Toniolo, R.; Dossi, N.; Svegelj, R.; Pigani, L.; Terzi, F.; Abollino, O.; Bontempelli, G. A deep eutectic solvent-based amperometric sensor for the detection of low oxygen contents in gaseous atmospheres. *Electroanalysis* **2016**, *28*, 757–763.
- Svigelj, R.; Dossi, N.; Grazioli, C.; Toniolo, R. Deep Eutectic Solvents (DESs) and Their Application in Biosensor Development. *Sensors* **2021**, *21*, 4263.
- Zainal-Abidin, M.; Hayyan, M.; Hayyan, A.; Jayakumar, N. New horizons in the extraction of bioactive compounds using deep eutectic solvents: a review. *Anal. Chim. Acta* **2017**, *979*, 1–23.
- Aroso, I. M.; Silva, J. C.; Mano, F.; Ferreira, A. S. D.; Dionísio, M.; Sá-Nogueira, I.; Barreiros, S.; Reis, R. L.; Paiva, A.; Duarte, A. R. C. Dissolution enhancement of active pharmaceutical ingredients by therapeutic deep eutectic systems. *Eur. J. Pharm. Biopharm.* **2016**, *98*, 57–66.
- Imteyaz, S.; Ingole, P. P. Comparison of physicochemical properties of choline chloride-based deep eutectic solvents for CO<sub>2</sub> capture: Progress and outlook. *J. Mol. Liq.* **2023**, *376*, No. 121436.
- Mota-Morales, J. D.; Sánchez-Leija, R. J.; Carranza, A.; Pojman, J. A.; del Monte, F.; Luna-Bárcenas, G. Free-radical polymerizations of and in deep eutectic solvents: green synthesis of functional materials. *Prog. Polym. Sci.* **2018**, *78*, 139–153.

- (16) Xu, P.; Zheng, G.-W.; Zong, M.-H.; Li, N.; Lou, W.-Y. Recent progress on deep eutectic solvents in biocatalysis. *Bioresour. Bioprocess.* **2017**, *4*, 34.
- (17) Sazali, A. L.; AlMasoud, N.; Amran, S. K.; Alomar, T. S.; Pa'ee, K. F.; El-Bahy, Z. M.; Yong, T-L. K.; Dailin, D. J.; Chuah, L. F. Physicochemical and thermal characteristics of choline chloride-based deep eutectic solvents. *Chemosphere*. **2023**, *338*, No. 139485.
- (18) Abbot, A. P. Deep eutectic solvents and their application in electrochemistry. *Curr. Opin. Green Sustainable Chem.* **2022**, *36*, No. 100649.
- (19) Boethling, R.; Sommer, E.; Difiore, D. Designing small molecules for biodegradability. *Chem. Rev.* **2007**, *107*, 2207–2227.
- (20) Kumar, N.; Gautam, R.; Stallings, J. D.; Coty, G. G.; Lynam, J. G. Secondary Agriculture Residues Pretreatment Using Deep Eutectic Solvents. *Waste and Biomass Valorization* **2021**, *12*, 2259–2269.
- (21) Huo, Z.; Fang, Y.; Yao, G.; Zeng, X.; Ren, D.; Jin, F. Improved two-step hydrothermal process for acetic acid production from carbohydrate biomass. *J. Energy Chem.* **2015**, *24*, 207–212.
- (22) Ng, M. H.; Abd. Hadi, N. Extraction of ferulic acid from oil palm pressed fiber by a choline chloride based deep eutectic solvent. *J. Am. Oil Chem. Soc.* **2022**, *99*, 443–453.
- (23) Kalhor, P.; Ghandi, K. Deep Eutectic Solvents for Pretreatment, Extraction, and Catalysis of Biomass and Food Waste. *Molecules*. **2019**, *24*, 4012.
- (24) García, G.; Aparicio, S.; Ullah, R.; Atilhan, M. Deep eutectic solvents: Physicochemical properties and gas separation applications. *Energy Fuels*. **2015**, *29*, 2616–2644.
- (25) Ribeiro, M. C. C. High viscosity of imidazolium ionic liquids with the hydrogen sulfate anion: A Raman spectroscopy study. *J. Phys. Chem. B* **2012**, *116*, 7281–7290.
- (26) Harifi-Mood, A. R.; Buchner, R. Density, viscosity, and conductivity of choline chloride + ethylene glycol as a deep eutectic solvent and its binary mixtures with dimethyl sulfoxide. *J. Mol. Liq.* **2017**, *225*, 689–695.
- (27) Ma, C.; Laaksonen, A.; Liu, C.; Lu, X.; Ji, X. The peculiar effect of water on ionic liquids and deep eutectic solvents. *Chem. Soc. Rev.* **2018**, *47*, 8685–8720.
- (28) Sheikh, A.; Saleem, I.; Ahmed, S.; Abbas, M.; Khan, A. Y. Investigation of physicochemical properties of NADES based on choline chloride and ascorbic acid and its binary solutions with DMSO from (298.15 to 353.15) K. *J. Mol. Liq.* **2022**, *364*, No. 120038.
- (29) Xie, Y.; Dong, H.; Zhang, S.; Lu, X.; Ji, X. Effect of water on the density, viscosity, and CO<sub>2</sub> solubility in choline chloride/urea. *J. Chem. Eng. Data* **2014**, *59*, 3344–3352.
- (30) Yadav, A.; Pandey, S. Densities and viscosities of (choline chloride + urea) deep eutectic solvent and its aqueous mixtures in the temperature range 293.15 to 363.15 K. *J. Chem. Eng. Data* **2014**, *59*, 2221–2229.
- (31) Yadav, A.; Trivedi, S.; Rai, R.; Pandey, S. Densities and dynamic viscosities of (choline chloride + glycerol) deep eutectic solvent and its aqueous mixtures in the temperature range (283.15–363.15) K. *Fluid Phase Equilib.* **2014**, *367*, 135–142.
- (32) Martin, D.; Weise, A.; Niclas, H. J. The solvent dimethyl sulfoxide. *Angew. Chem., Int. Ed. Engl.* **1967**, *6*, 318–334.
- (33) Luyben, W. L. Effect of Solvent on Controllability in Extractive Distillation. *Ind. Eng. Chem. Res.* **2008**, *47*, 4425–4439.
- (34) Zhuchkov, V.; Raeva, V.; Frolkova, A. Densities and excess volumes of binary and ternary mixtures of N, N-dimethyl sulfoxide, N, N-dimethylacetamide, and N-methyl-2-pyrrolidone at T = (293.15, 313.15) K and atmospheric pressure. *Chem. Data Coll.* **2022**, *38*, No. 100840.
- (35) Troter, D.; Todorovic, Z.; Djokic-Stojanovic, D.; Djordjevic, B.; Todorovic, V.; Konstantinovic, S.; Veljkovic, V. The physico-chemical and thermodynamic properties of the choline chloride-based deep eutectic solvents. *J. Serb. Chem. Soc.* **2017**, *82*, 1039–1052.
- (36) Shah, D.; Mansurov, U.; Mjalli, F. S. Intermolecular interactions and solvation effects of dimethylsulfoxide on type III deep eutectic solvents. *Phys. Chem. Chem. Phys.* **2019**, *21*, 17200–17208.
- (37) Kim, K.-S.; Park, B. H. Volumetric properties of solutions of choline chloride + glycerol deep eutectic solvent with water, methanol, ethanol or iso-propanol. *J. Mol. Liq.* **2018**, *254*, 272–279.
- (38) Haghbaksh, R.; Raeissi, S. Densities and volumetric properties of (choline chloride+urea) deep eutectic solvent and methanol mixtures in the temperature range of 293.15–323.15 K. *J. Chem. Thermodyn.* **2018**, *124*, 10–20.
- (39) Abbas, Q.; Binder, L. Synthesis and characterization of choline chloride based binary mixtures. *ECS Trans.* **2010**, *33*, 49–59.
- (40) Sethi, O.; Singh, M.; Kang, T. S.; Sood, A. K. Volumetric and compressibility studies on aqueous mixtures of deep eutectic solvents based on choline chloride and carboxylic acids at different temperatures: Experimental, theoretical and computational approach. *J. Mol. Liq.* **2021**, *340*, No. 117212.
- (41) Zhang, J.; Yin, J.; Zhang, Y.; Zhu, T.; Ran, H.; Jiang, W.; Li, H.; Li, H.; Zhang, M. Insights into the formation mechanism of aliphatic acid-choline chloride deep eutectic solvents by theoretical and experimental research. *J. Mol. Liq.* **2022**, *367*, No. 120342.
- (42) Shekaari, H.; zafarani-Moattar, M. T.; Mokhtarpour, M.; Faraji, S. Volumetric and compressibility properties for aqueous solutions of choline chloride based deep eutectic solvents and Prigogine–Flory–Patterson theory to correlate excess molar volumes at T = (293.15 to 308.15) K. *J. Mol. Liq.* **2019**, *289*, No. 111077.
- (43) Kuddushi, M.; Nangala, G. S.; Rajput, S.; Ijaardar, S. P.; Malek, N. I. Understanding the peculiar effect of water on the physicochemical properties of choline chloride based deep eutectic solvents theoretically and experimentally. *J. Mol. Liq.* **2019**, *278*, 607–615.
- (44) Domańska, U.; Laskowska, M. Temperature and Composition Dependence of the Density and Viscosity of Binary Mixtures of {1-Butyl-3-methylimidazolium Thiocyanate + 1-Alcohols}. *J. Chem. Eng. Data* **2009**, *54*, 2113–2119.
- (45) Ramkumar, V.; Gardas, R. L. Exploring the solvation behavior of guanidinium based carboxylate ionic liquids in DMSO and DMF through apparent molar properties. *J. Mol. Liq.* **2021**, *323*, No. 117664.
- (46) Agieienko, V.; Buchner, R. Variation of Density, Viscosity and Electrical Conductivity of the Deep Eutectic Solvent Reline, Composed of Choline Chloride and Urea at Molar Ratio 1:2, Mixed with Dimethylsulfoxide as a Co-solvent. *J. Chem. Eng. Data* **2020**, *65*, 1900–1910.
- (47) Wang, Y.; Ma, C.; Liu, C.; Lu, X.; Feng, X.; Ji, X. Thermodynamic study of choline chloride-based deep eutectic solvents with water and methanol. *J. Chem. Eng. Data* **2020**, *65*, 2446–2457.
- (48) Palaiologou, M. M.; Arianas, G. K.; Tsierkezos, N. G. Thermodynamic Investigation of Dimethyl Sulfoxide Binary Mixtures at 293.15 and 313.15 K. *J. Solution Chem.* **2006**, *35*, 1551–1565.
- (49) Treszczanowicz, A. J.; Benson, G. C. Excess volumes for n-alkanols + n-alkanes II. Binary mixtures of n-pentanol, nhexanol, n-octanol, and n-decanol + n-heptane. *J. Chem. Thermodyn.* **1978**, *10*, 967–974.
- (50) Ali, A.; Nain, A. K.; Sharma, V. K.; Ahmad, S. Molecular interactions in binary mixtures of tetrahydrofuran with alkanols (C<sub>6</sub>, C<sub>8</sub>, C<sub>10</sub>): an ultrasonic and volumetric study. *Indian J. Pure Appl. Phys.* **2004**, *42*, 666–673.
- (51) Zhao, T.; Zhang, J.; Guo, B.; Zhang, F.; Sha, F.; Xie, X.; Wei, X. Density, viscosity and spectroscopic studies of the binary system of ethylene glycol + dimethyl sulfoxide at T = (298.15 to 323.15) K. *J. Mol. Liq.* **2015**, *207*, 315–322.
- (52) Azarang, N.; Movagharnejad, K.; Piradshti, M.; Ketabi, M. Densities, Viscosities, and Refractive Indices of Poly (ethylene glycol) 300 + 1,2-Ethanediol, 1,2-Propanediol, 1,3-Propanediol, 1,3-Butanediol, or 1,4-Butanediol Binary Liquid Mixtures. *J. Chem. Eng. Data* **2020**, *65*, 3448–3462.
- (53) Malloum, A.; Conradie, J. Conradie, J. Dimethylsulfoxide (DMSO) clusters dataset: DFT relative energies, non-covalent

- interactions, and cartesian coordinates. *Data Brief* **2022**, *42*, No. 108024.
- (54) Venkataramanan, N. S.; Suvitha, A. Nature of bonding and cooperativity in linear DMSO clusters: A DFT, AIM and NCI analysis. *J. Mol. Graph. Model.* **2018**, *81*, 50–59.
- (55) Forel, M.-T.; Tranquille, M. Spectres de vibration du diméthylsulfoxyde et du diméthylsulfoxyde-*d*<sub>6</sub>. *Spectrochim Acta Part A: Molecular spectroscopy*. **1970**, *26*, 1023–1034.
- (56) Skripkin, M. Y.; Lindqvist-Reis, P.; Abbasi, A.; Mink, J.; Persson, I.; Sandström, M. Vibrational spectroscopic force field studies of dimethyl sulfoxide and hexakis(dimethyl sulfoxide)-scandium(iii) iodide, and crystal and solution structure of the hexakis(dimethyl sulfoxide)scandium(iii) ion. *Dalton Trans.* **2004**, *23*, 4038–4049.
- (57) Ye, F.; Zhu, J.; Yu, K.; Zhu, R.; Xu, Y.; Chen, J.; Chen, L. Physicochemical properties of binary mixtures of 1,1,3,3-tetramethylguanidine imidazolidine ionic liquid with water and alcohols. *J. Chem. Thermodyn.* **2016**, *97*, 39–47.
- (58) Zhao, Z.; Dong, Y.; Liu, X.; Qin, X.; Wu, J.; Zhang, J.; Wu, Z. Density, viscosity, refractive index and molecular interaction of polyethylene glycol 400 + 1,3-propanediamine deep eutectic solvent for CO<sub>2</sub> capture. *J. Mol. Liq.* **2022**, *367*, No. 120542.
- (59) Redlich, O.; Kister, A. T. Thermodynamics of non-electrolyte solutions, x-y-t relation in binary system. *Ind. Eng. Chem.* **1948**, *40*, 341–345.
- (60) Ijardar, S. P. Deep eutectic solvents composed of tetrabutylammonium bromide and PEG: density, speed of sound and viscosity as a function of temperature. *J. Chem. Thermodyn.* **2020**, *140*, No. 105897.
- (61) Douhéret, G.; Davis, M. I.; Reis, J. C.; Blandamer, M. J. Isentropic Compressibilities - Experimental Origin and the Quest for their Rigorous Estimation in Thermodynamically Ideal Liquid Mixtures. *Chemphyschem*. **2001**, *2*, 148–161.
- (62) Wu, K.-J.; Chen, Q.-L.; He, C.-H. Speed of sound of ionic liquids: database, estimation, and its application for thermal conductivity prediction. *AIChE J.* **2014**, *60*, 1120–1131.
- (63) Sánchez, P. B.; González, B.; Salgado, J.; Parajó, J. J.; Domínguez, Á. Physical properties of seven deep eutectic solvents based on L-proline or betaine. *J. Chem. Thermodyn.* **2019**, *132*, 517–523.
- (64) Mjalli, F. S.; Abdel Jabbar, N. M. Acoustic investigation of choline chloride based ionic liquids analogs. *Fluid Phase Equilib.* **2014**, *381*, 71–76.
- (65) Omar, K. A.; Sadeghi, R. Novel Deep Eutectic Solvents Based on Pyrogallol: Synthesis and Characterizations. *J. Chem. Eng. Data* **2021**, *66*, 2088–2095.
- (66) Rama Rao, P. V. S. S.; Krishna, T. S.; Bharath, P.; Dey, R.; Ramachandran, D. Understanding of molecular interactions between ethyl acetate and 1-butyl-3-methyl-imidazolium bis (trifluoromethylsulfonyl) imide: A thermophysical study. *J. Chem. Thermodyn.* **2021**, *156*, No. 106383.
- (67) Keshapolla, D.; Srinivasarao, K.; Gardas, R. L. Influence of temperature and alkyl chain length on physicochemical properties of trihexyl- and trioctylammonium based protic ionic liquids. *J. chem. Thermodyn.* **2019**, *133*, 170–180.
- (68) Marcinkowski, Ł.; Szepiński, E.; Milewska, M. J.; Kłoskowski, A. Density, sound velocity, viscosity, and refractive index of new morpholinium ionic liquids with amino acid-based anions: Effect of temperature, alkyl chain length, and anion. *J. Mol. Liq.* **2019**, *284*, 557–568.
- (69) Chand, G. P.; Sankar, M. G.; Rani, P. N. V. V. L. P.; Rambabu, C. Studies of intermolecular interactions in binary mixtures of 2-chloroaniline with selected di- and tri-substituted benzenes. *J. Mol. Liq.* **2015**, *201*, 1–9.
- (70) Sunkara, G. R.; Tadavarthi, M. M.; Tadekoru, V. K.; Tadikonda, S. K.; Bezwada, S. R. Density, Refractive Index, and Speed of Sound of the Binary Mixture of 1-Butyl-3-methylimidazolium Tetrafluoroborate + N-Vinyl-2-pyrrolidinone from T = (298.15 to 323.15) K at Atmospheric Pressure. *J. Chem. Eng. Data* **2021**, *60*, 886–894.
- (71) Saini, A.; Prabhune, A.; Mishra, A. P.; Dey, R. Density, ultrasonic velocity, viscosity, refractive index and surface tension of aqueous choline chloride with electrolyte solutions. *J. Mol. Liq.* **2021**, *323*, No. 114593.
- (72) Pandey, J. D.; Dey, R.; Chhabra, J. Thermoacoustical approach to the intermolecular free length of liquid mixtures. *PhysChemComm.* **2003**, *6*, 55–58.
- (73) Jacobson, B. Ultrasonic Velocity in Liquids and Liquid Mixtures. *J. Chem. Phys.* **1952**, *20*, 927–928.
- (74) Praharaj, M.; Satapathy, A.; Mishra, P.; Mishra, S. Ultrasonic studies of ternary liquid mixtures of N-N-dimethylformamide, nitrobenzene, and cyclohexane at different frequencies at 318 K. *J. Theor. Appl. Phys.* **2013**, *7*, 23.
- (75) Thakur, A.; Anand, V.; Kumari, A. Inter-molecular investigation of polyethylene glycols in methanol and butylparaben mixture to compute volumetric and acoustic parameters at 293.15 & 298.15 k temperature. *J. Phys.: Conf. Ser.* **2022**, *2267*, No. 012099.
- (76) Haghbakhsh, R.; Parvaneh, K.; Raeissi, S.; Shariati, A. A general viscosity model for deep eutectic solvents: The free volume theory coupled with association equations of state. *Fluid Phase Equilib.* **2018**, *470*, 193–202.
- (77) Al-Dawsari, J. N.; Bessadok-Jemai, A.; Wazeer, I.; Mokraoui, S.; AlMansour, M. A.; Hadj-Kali, M. K. Fitting of experimental viscosity to temperature data for deep eutectic solvents. *J. Mol. Liq.* **2020**, *310*, No. 113127.
- (78) Perna, F. M.; Vitale, P.; Capriati, V. Deep eutectic solvents and their applications as green solvents. *Curr. Opin. Green Sustain.* **2020**, *21*, 27–33.
- (79) Jangir, A. K.; Lad, B.; Dani, U.; Shah, N.; Kuperkar, K. In vitro toxicity assessment and enhanced drug solubility profile of green deep eutectic solvent derivatives (DESDs) combined with theoretical validation. *RSC Adv.* **2020**, *10*, 24063–24072.
- (80) Pei, Y.; Zhang, W.; Zhang, Y.; Ma, J.; Zhao, Y.; Li, Z.; Wang, J.; Du, R. Physicochemical properties and thermal-responsive phase separation of poly (ethylene glycol)-based ionic liquids. *J. Mol. Liq.* **2022**, *360*, No. 119471.
- (81) Hecksher, T.; Nielsen, A.; Olsen, N.; Dyre, J. C. Little evidence for dynamic divergences in ultraviscous molecular liquids. *Nat. Phys.* **2008**, *4*, 737–741.
- (82) Shekaari, H.; Zafarani-Moattar, M. T.; Mohammadi, B. Thermophysical characterization of aqueous deep eutectic solvent (choline chloride/urea) solutions in full ranges of concentration at T = (293.15–323.15) K. *J. Mol. Liq.* **2017**, *243*, 451–461.
- (83) Mahajan, A. R.; Mirgane, S. R. Excess Molar Volumes and Viscosities for the Binary Mixtures of n-Octane, n-Decane, n-Dodecane, and n-Tetradecane with Octan-2-ol at 298.15 K. *J. Thermodyn.* **2013**, *2013*, 1–11.
- (84) Lemaoui, T.; Darwish, A. S.; Hammoudi, N. E. H.; Hatab, F. A.; Attou, A.; Alnashef, I. M.; Benguerba, Y. Prediction of Electrical Conductivity of Deep Eutectic Solvents Using COSMO-RS Sigma Profiles as Molecular Descriptors: A Quantitative Structure–Property Relationship Study. *Ind. Eng. Chem. Res.* **2020**, *59*, 13343–13354.
- (85) El Achkar, T.; Greige-Gerges, H.; Fourmentin, S. Basics and properties of deep eutectic solvents: a review. *Environ. Chem. Lett.* **2021**, *19*, 3397–3408.
- (86) Casteel, J. F.; Amis, E. S. Specific conductance of concentrated solutions of magnesium salts in water-ethanol system. *J. Chem. Eng. Data* **1972**, *17*, 55–59.
- (87) Stoppa, A.; Hunger, J.; Buchner, R. Conductivities of Binary Mixtures of Ionic Liquids with Polar Solvents. *J. Chem. Eng. Data* **2009**, *54*, 472–479.
- (88) Zhang, Q.-G.; Sun, S.-S.; Pitula, S.; Liu, Q.-S.; Welz-Biermann, U.; Zhang, J.-J. Electrical Conductivity of Solutions of Ionic Liquids with Methanol, Ethanol, Acetonitrile, and Propylene Carbonate. *J. Chem. Eng. Data* **2011**, *56*, 4659–4664.

- (89) Every, H.; Bishop, A. G.; Forsyth, M.; MacFarlane, D. Ion diffusion in molten salt mixtures. *Electrochim. Acta* **2000**, *45*, 1279–1284.